Quasi-Elastic Light-Scattering Studies of Aqueous Biliary Lipid Systems. Cholesterol Solubilization and Precipitation in Model Bile Solutions†

Norman A. Mazer* and Martin C. Carey

ABSTRACT: We have employed quasi-elastic light-scattering methods to characterize micellar aggregates and microprecipitates formed in aqueous solutions containing sodium taurocholate (TC), egg lecithin (L), and cholesterol (Ch). Particle size and polydispersity were studied as functions of Ch mole fraction (X_{Ch} = 0–15%), L/TC molar ratio (0–1.6), temperature (5–85 °C), and total lipid concentration (3 and 10 g/dL in 0.15 M NaCl). For X_{Ch} values below the established solubilization limits (X_{Ch}^{max}) [Carey, M. C., & Small, D. M. (1978) *J. Clin. Invest. 61*, 998], added Ch has little influence on the size of simple TC micelles (type 1 systems), on the coexistence of simple and mixed TC–L micelles (type 2 systems), or on the growth of "mixed disc" TC–L micelles (type 3 systems). For supersaturated systems ($X_{Ch}/X_{Ch}^{max} > 1$), 10 g/dL type 1 systems (L/TC = 0) exist as metastable micellar solutions even at $X_{Ch}/X_{Ch}^{max} = 5.3$. Metastability is decreased in type 2 systems ($0 < L/TC < 0.6$), and "labile" microprecipitation occurs when X_{Ch}/X_{Ch}^{max} exceeds ~1.6. In 10 g/dL mixtures, the microprecipitates initially range in size from 500 to 20 000 Å and later coalesce to form a buoyant macroscopic precipitate phase. In 3 g/dL mixtures, the microprecipitates are smaller (200–400 Å) and remain as a stable, noncoalesced microdispersion. Transmission electron microscopy of the microprecipitates formed at both concentrations indicates a globular noncrystalline structure, and lipid analysis reveals the presence of cholesterol and lecithin in a molar ratio (Ch/L) of approximately 2/1, suggesting that the microprecipitates represent a metastable cholesterol-rich liquid-crystalline phase. In supersaturated type 3 systems ($0.6 < L/TC < 2.0$), the precipitate phase is a lecithin-rich liquid-crystalline phase which likewise coalesces in a 10 g/dL system but forms stable vesicle (liposomal) structures (600–800 Å radius) in 3 g/dL systems. In conjunction with these experimental data, we present a quantitative thermodynamic analysis of Ch solubilization in model bile systems from which rigorous deductions of the free energy and enthalpy change for solubilization of cholesterol monohydrate in type 1 and type 2 systems are obtained. In addition, we employ homogeneous nucleation theory to analyze the origin of the metastable/labile limit in supersaturated systems and to deduce the interfacial tension between microprecipitates and solution. On the basis of these experimental data and theoretical analyses, we offer new hypotheses on the structure and physiology of bile and the pathogenesis of Ch gallstones. In particular, it is suggested that the "stable" microprecipitates observed in 3 g/dL type 2 systems may provide a secondary vehicle (in addition to micelles) for cholesterol transport in supersaturated hepatic bile.

Although the aqueous monomeric solubility of cholesterol (Ch)[1] monohydrate is less than 10^{-7} M (Saad & Higuchi, 1965), appreciable amounts ($>10^{-3}$ M) can be solubilized in aqueous bile salt and bile salt–lecithin solutions by being incorporated within micellar aggregates (Bourgès et al., 1967; Carey & Small, 1970, 1978). It is by such micellar solubilization that all three biliary lipids are believed to be transported within hepatic bile (Small, 1967; Hardison & Apter, 1972) and by which they normally remain in solution within the gallbladder, where the total lipid concentration of bile increases 3–10-fold as a result of water resorption (Forker, 1979). However, when the relative amount of cholesterol in either native bile or model biliary lipid systems exceeds the limit of micellar solubilization, a state of supersaturation exists and may ultimately result in the precipitation of insoluble phases containing the excess cholesterol (Bourgès et al., 1967; Holzbach & Marsh, 1975; Carey & Small, 1978). The hepatic production of supersaturated bile, followed by its precipitation in the gallbladder, is now recognized as an essential sequence in the pathophysiology of cholesterol gallstones (Small, 1967; Admirand & Small, 1968; Shaffer & Small, 1976).

Because of the relevance of cholesterol solubilization and precipitation to understanding the physical chemistry of bile and cholesterol gallstone formation, the phase equilibria of aqueous biliary lipid systems have been extensively investigated (Bourgès et al., 1967; Holzbach et al., 1973; Carey & Small, 1978). At present, however, experimental and theoretical information concerning the molecular, thermodynamic, and kinetic aspects of these phase equilibria remains sparse. For this reason, we have employed the technique of quasi-elastic light scattering (QLS) to determine the mean hydrodynamic radius ($\bar{R}_h$) and polydispersity of the micellar aggregates and microprecipitates formed in unsaturated and supersaturated biliary lipid systems. The present work thus extends our previous QLS investigations of aqueous bile salt (Mazer et al., 1979; Carey et al., 1981) and bile salt–lecithin (Mazer et al., 1980) solutions by studying the effects of cholesterol incorporation in these model bile systems. Of particular note is our attempt in this work to compare and contrast the properties of model bile solutions containing two total lipid concentrations (3 and 10 g/dL) typical of hepatic and gallbladder biles, respectively (Carey and Small, 1978). From our experimental results and theoretical analyses, we offer new insights into the molecular interactions of the biliary lipids and the possible role

† From the Department of Medicine, Harvard Medical School, Division of Gastroenterology, Brigham and Women's Hospital, Boston, Massachusetts 02115, and the Department of Physics, Center for Material Science and Engineering, Massachusetts Institute of Technology, Cambridge, Massachusetts 02139. *Received March 22, 1982.* Supported in part by National Science Foundation Grants DMR-78-24185 and CHE-77-07666, NIAMDD Grant AM-18559, and RCDA Grant AM-00195 (to M.C.C.).

* Correspondence should be addressed to this author (in care of Dr. Martin C. Carey) at the Department of Medicine, Brigham and Women's Hospital.

[1] Abbreviations: QLS, quasi-elastic light scattering; BS, bile salt; TC, taurocholate; L, lecithin; Ch, cholesterol; X_{Ch}, cholesterol mole fraction; L/BS, lecithin to bile salt molar ratio; TEM, transmission electron microscopy; $\bar{R}_h$, mean hydrodynamic radius; $NaDodSO_4$, sodium dodecyl sulfate.

0006-2960/83/0422-0426$01.50/0

of these phenomena in the physiology of bile and the pathogenesis of cholesterol gallstones.

Experimental Procedures

(*A*) *Materials.* Cholesterol (Ch) was obtained from Nu-Chek Prep (Austin, MN) and was recrystallized 3 times from hot ethanol and stored at 4 °C under nitrogen. Its purity (>99.5%) was checked by thin-layer chromatography, hot-stage microscopy, and differential scanning calorimetry. Egg lecithin (L), sodium taurocholate, and aqueous solvents were identical with those used previously (Mazer et al., 1979, 1980). Deuterium oxide (D_2O) was obtained from MSD Isotopes (Rahway, NJ).

(*B*) *Solutions.* (*1*) *Methods of Preparation. Path A.* In the principal method of sample preparation (designated path A), aqueous TC–L–Ch solutions, having a particular L/TC molar ratio and Ch mole fraction (X_{Ch}), were made by the method of coprecipitation (Carey & Small, 1978; Mazer et al., 1980) from chloroform–methanol (1:1) or ethanol solvents. The desired total lipid concentration (either 3 or 10 g/dL) was then obtained by adding aqueous solvent (0.15 M NaCl, pH 6–7) to the dried lipid film, after which the samples were flushed with purified N_2, sealed, and equilibrated at room temperature (room temperature = 22 ± 1 °C) for at least 2 days with periodic vortex mixing. Other "paths" (B, C, and D) of sample preparation were used for making supersaturated systems containing 3 g/dL total lipids, L/TC = 0.4, and X_{Ch} = 10% (equivalent to 1.78 g/dL TC, 1.02 g/dL L, and 0.20 g/dL Ch).

Path B. A 10 g/dL solution with L/TC = 0.4 and X_{Ch} = 10% prepared by path A was heated to 70 °C for 1 h, then diluted to 3 g/dL with 0.15 M NaCl at the same temperature, and finally equilibrated at room temperature for 24 h.

Path C. A 3 g/dL TC–L solution (L/TC = 0.4) prepared by path A was mixed with cholesterol monohydrate crystals (Igimi & Carey, 1981) to attain X_{Ch} = 10%, flushed with N_2, and equilibrated at room temperature for 2 days with periodic vortex mixing. The sample was then divided into two aliquots, C1 and C2; the former was kept at room temperature, while the latter was incubated for 3 h at 90 °C. Sample C2 was then cooled to room temperature for 1 h prior to investigation. Mixtures prepared by paths C1 and, to a lesser extent, C2 contained some insoluble cholesterol.

Path D. A coprecipitated L–Ch film (L/Ch molar ratio = 0.39) was first hydrated in 0.15 M NaCl (path D1) to form a liquid-crystalline dispersion (total lipid concentration 2.44 g/dL) and equilibrated at room temperature for 24 h. An equal volume of TC solution (3.56 g/dL in 0.15 M NaCl) was then added, and the mixture was further equilibrated for 24 h with periodic vortex mixing. In path D2, an identical L–Ch film was hydrated directly with TC solution (1.78 g/dL in 0.15 M NaCl) to give a total lipid concentration of 3 g/dL and equilibrated at room temperature for 48 h. By both paths, the resulting solutions contained residual amounts of liquid-crystalline precipitate which were separated from the supernatant phases by centrifugation (10000*g* for 20 min).

(*2*) *Thermal History of Samples.* Samples prepared by path A contained one or more macroscopic phases that separated under gravity, depending on the relative and total lipid compositions. Small aliquots (0.5 mL) of the single-phase systems were pipetted into light-scattering cells (Kimble cylindrical tubes, 6 × 5 mm), centrifuged (10000*g* for 20 min at 20 °C) in order to sediment dust, and then kept at room temperature. Multiphase systems were first incubated at high temperatures (60–95 °C) for up to 3 h in an attempt to solubilize the precipitated phases. When successful, 0.5-mL aliquots were placed in preheated scattering cells, centrifuged (10000*g* for 10 min) at high temperatures (>60 °C), and immediately studied or reincubated at high temperature. Careful inspection of the samples revealed no significant precipitation during the centrifugation. When high-temperature incubation did not solubilize the precipitate phases, the two-phase systems were vortex mixed, and 0.5-mL aliquots were placed in scattering cells. After equilibration at room temperature for 48 h, the samples were centrifuged at moderate speed (10000*g* for 30–60 min at 20 °C) in a fixed-angle rotor (Beckman Model J 21B) to separate the phases. The scattering cells were then aligned with respect to the laser beam so that only the supernatant phase was illuminated.

Thermal control of the scattering cell was maintained by a Peltier thermoelectric heating and cooling device which enabled us to vary the temperature of the sample between 0 and 100 °C with a thermal equilibration time of approximately 4 min. Under conditions where a temperature change T_i (initial temperature) → T_f (final temperature) resulted in microprecipitation, the samples were continuously studied until an apparent quiescence had occurred and were then returned to T_i.

(*C*) *Methods.* (*1*) *Quasi-Elastic Light Scattering* (*QLS*). (*a*) *Autocorrelation Functions.* QLS measurements of the autocorrelation function of light scattered from aqueous biliary lipid systems were performed by using the same apparatus, data acquisition methods, and data analysis as described in the preceding papers (Mazer et al., 1979, 1980), with the addition of a 56-channel autocorrelator (NICOMP Instruments 6864), operating in the delayed base-line mode. From these measurements, determinations of the mean translational diffusion coefficient ($\bar{D}$) and micellar polydispersity parameter (V) were obtained, using the cumulant analysis (Koppel, 1972; Mazer et al., 1976, 1980).

From the $\bar{D}$ values, the apparent mean hydrodynamic radius of the particles, $\bar{R}_h$, was deduced by using the Stokes–Einstein relation [see Mazer et al. (1976) and Missel et al. (1980)]. Such deductions assume the influences of interparticle interactions on $\bar{D}$ to be small, an assumption which has been verified for TC micelles at the lipid concentrations and ionic strengths employed (Mazer, 1978; Mazer et al., 1979). The quantitative relation of $\bar{R}_h$ and V to the distribution of particle sizes and shapes is given elsewhere (Missel et al., 1980).

(*b*) *Scattered Intensity Measurements.* The time-averaged intensity of the scattered light ($\bar{I}$) at the scattering angle (θ = 90°) was obtained by measuring the photomultiplier tube output, using a digital current meter (Mazer et al., 1979). The time dependence, $\bar{I}(t)/[\bar{I}(0)]$, was used to quantify the response of biliary lipid systems to temperature changes ($T_i \rightarrow T_f$) in which supersaturation of varying degrees was created to produce microprecipitation. Systems in which $\bar{I}(t)/[\bar{I}(0)]$ remained constant for at least 1 h were termed *metastable*, whereas systems in which changes occurred within 1 h were termed *labile*. When $\bar{I}(t)/[\bar{I}(0)]$ was slowly varying, it was possible to measure the autocorrelation function and thereby deduce $\bar{R}_h$ and V for the microprecipitates.

(*c*) *Angular Dissymmetry Measurements.* In certain cases, the angular dissymmetry of the scattered light, $I(\theta)/[I(180° - \theta)]$ was measured in order to deduce the mean radius of gyration of the macromolecules ($\bar{R}_g$) by using the apparatus described by Young et al. (1978). Comparison of $\bar{R}_g$ with $\bar{R}_h$ provided insights into the shape and possible structure of the aggregates (Young et al., 1978).

(*2*) *Transmission Electron Microscopy* (*TEM*). TEM of microprecipitates formed in two supersaturated biliary lipid

systems was performed by using conventional staining techniques (Hall, 1953) and the apparatus employed previously (Mazer et al., 1980). Sample 1 (10 g/dL total lipids, L/TC ratio = 0.25, and X_{Ch} = 10%) was cooled from 60 to 20 °C for 30 min to produce microprecipitates. Sample 2 (3 g/dL total lipids, L/TC = 0.4, and X_{Ch} = 10%) was incubated at room temperature for 2 days to produce microprecipitates. Magnification was approximately 50000× in both cases.

(3) Biliary Lipid Analyses. Lipid analyses for TC, L, and Ch were performed by using standard methods (Carey & Small, 1978; Fromm et al., 1980; Gurantz et al., 1981; Igimi & Carey, 1981) on different supersaturated systems prepared as follows:

(a) Aliquots (0.5 mL) of four samples (10 g/dL total lipids, L/TC = 0.25, and X_{Ch} = 7.5%, 8.5%, 10%, and 12%) were initially heated to 80 °C to solubilize all the cholesterol and then cooled to 4 °C for 30 min to produce turbid suspensions. Centrifugation (10000*g* for 60 min at 20 °C) separated the microprecipitated material from solution as a buoyant opaque film. The infranatant micellar phases were carefully aspirated by using a hypodermic syringe, and the precipitate films were dissolved in absolute ethanol. Biliary lipid analyses of the stock solutions and infranatant and precipitate phases were determined as milligram of lipid per aliquot of sample.

(b) A 3 g/dL supersaturated system (L/TC = 0.4, X_{Ch} = 10%) containing microprecipitates was first diluted with an equal volume of 0.15 M NaCl in D_2O. Aliquots (4 mL) were then ultracentrifuged at 240000*g* for 25 h (20 °C) in an SW 50.1 swinging-bucket rotor (Beckman Model L5-65 ultracentrifuge) which produced a thin (~1 mm) turbid upper phase and a clear infranatant phase. Both phases were harvested as described above, and their biliary lipid compositions were analyzed.

(c) Turbid solutions (3 g/dL total lipids, L/TC = 1.2, X_{Ch} = 7.5% and 10%) separated into precipitate and clear supernatant phases after centrifugation (10000*g* for 20 min at 20 °C). Both phases were isolated and analyzed as in the previous cases.

Results

(A) Cholesterol Solubilization: Influence on Micellar Sizes and Polydispersity. We briefly summarize relevant background information concerning (1) the limits of cholesterol solubilization in taurocholate–egg lecithin solutions (Carey & Small, 1978) and (2) the properties of TC micelles and TC–L mixed micelles without Ch deduced by QLS studies (Mazer et al., 1980). In panels A and B of Figure 1, the dependence of the solubilization limit (expressed as the Ch mole fraction, X_{Ch}^{max}) on the lecithin to bile salt molar ratio (L/BS) has been plotted at various temperatures (24–80 °C) for TC–L–Ch solutions (0.15 M NaCl) whose total lipid concentrations are 10 and 3 g/dL, respectively. Systems with Ch mole fractions (X_{Ch}) falling below the X_{Ch}^{max} curves correspond to single-phase micellar solutions, whereas systems with $X_{Ch} > X_{Ch}^{max}$ contain additional precipitate phases composed of Ch and/or L (Carey & Small, 1978). As seen in Figure 1A, the micellar phase boundary increases markedly as a function of temperature at low L/BS ratios (0–0.5), while at high L/BS ratios (greater than 1.0), it diminishes with temperature elevation. These temperature effects have been utilized in the present work as a means for incorporating the maximal amounts of Ch into the micellar phase at various L/BS ratios and also for investigating the kinetic behavior of supersaturated systems in response to temperature changes (see section B under Results). Also indicated in Figure 1A,B are the types of micelles which form at different L/BS ratios in bile salt–lecithin solutions without Ch, as deduced from their mean hydrodynamic radius ($\bar{R}_h$) and polydispersity parameter (V) (Mazer et al., 1980). Type 1 systems (L/BS = 0) contain simple TC micelles ($\bar{R}_h$ = 10–12 Å, $V \simeq$ 30%). Type 2 systems (0 < L/BS < 0.6) contain simple micelles which coexist in varying proportions with small mixed micelles of nearly fixed composition (L/BS ≃ 0.6), size ($\bar{R}_h \simeq$ 20–30 Å), and polydispersity ($V \simeq$ 25%). Type 3 systems (0.6 < L/BS < phase limit) contain only mixed BS–L micelles whose size and polydispersity increase markedly as the L/BS ratio approaches the L solubilization limit ($\bar{R}_h \simeq$ 20 Å to greater than 200 Å, $V \simeq$ 25% to greater than 50%). The structure of these mixed micelles has been shown to be quantitatively consistent with a "mixed disc" model (Mazer et al., 1980; Müller, 1981).

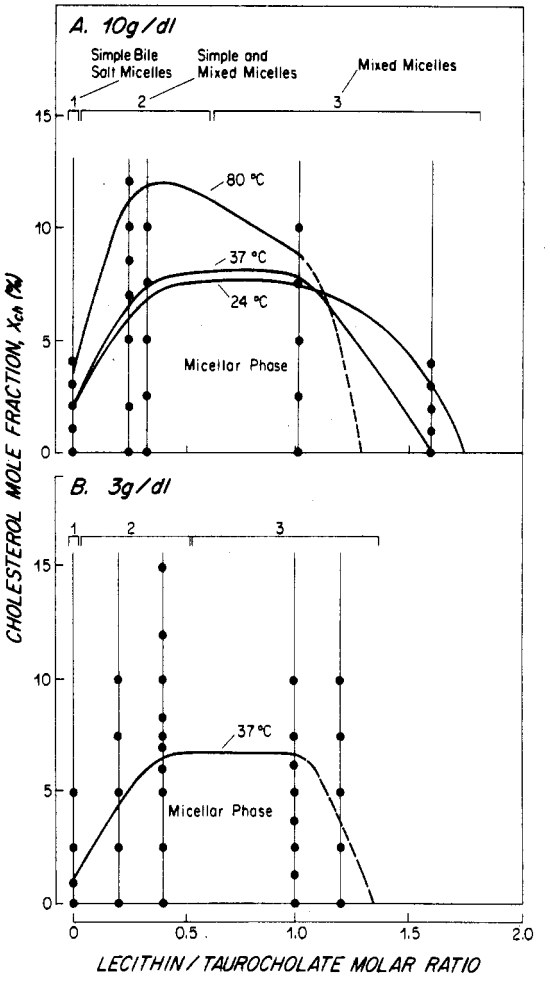

FIGURE 1: Cholesterol solubilization limits (micellar phase boundaries) in taurocholate (TC)–lecithin (L)–cholesterol (Ch) systems, expressed as the cholesterol mole fraction and plotted as a function of the L/TC molar ratio. Total lipid concentration is 10 g/dL in (A) and 3 g/dL in (B). Solid curves are derived from the phase diagrams of Carey & Small (1978), obtained at various temperatures (24–80 °C). Broken curves are extrapolated to the known limits of lecithin solubilization (Mazer et al., 1980). Solid circles indicate compositions of mixtures investigated by QLS. Horizontal bars denote ranges of L/TC ratios where type 1, 2, and 3 micellar systems exist. See text for details.

In the following sections, we present results of the influence of solubilized Ch on the apparent mean size ($\bar{R}_h$) and polydispersity (V) of micelles formed in type 1, 2, and 3 systems in both 10 and 3 g/dL solutions at various temperatures. The compositions studied are indicated by solid circles in Figure 1A,B and were chosen to span the entire micellar phase.

(1) Type 1 Systems: Ch Solubilization in Simple TC Micelles. Panels A and B of Figure 2 show the dependence of $\bar{R}_h$ on X_{Ch} for type 1 solutions containing 10 and 3 g/dL

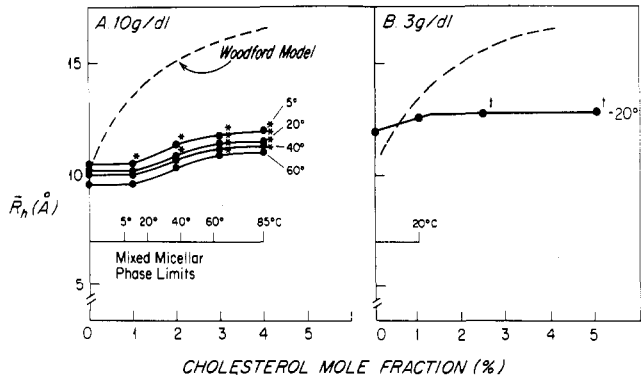

FIGURE 2: Mean hydrodynamic radii, $\bar{R}_h$ (angstroms), plotted as a function of the cholesterol mole fraction (percent) in type 1 micellar systems at various temperatures. Total lipid concentration is 10 g/dL in (A) and 3 g/dL in (B). Asterisks indicate metastably supersaturated systems whose cholesterol content exceeds the micellar phase limit. Daggers indicates two-phase systems in which the $\bar{R}_h$ value corresponds to the supernatant micellar phase. The broken curve is a theoretical prediction of $\bar{R}_h$ based on Woodford's model (Woodford, 1969).

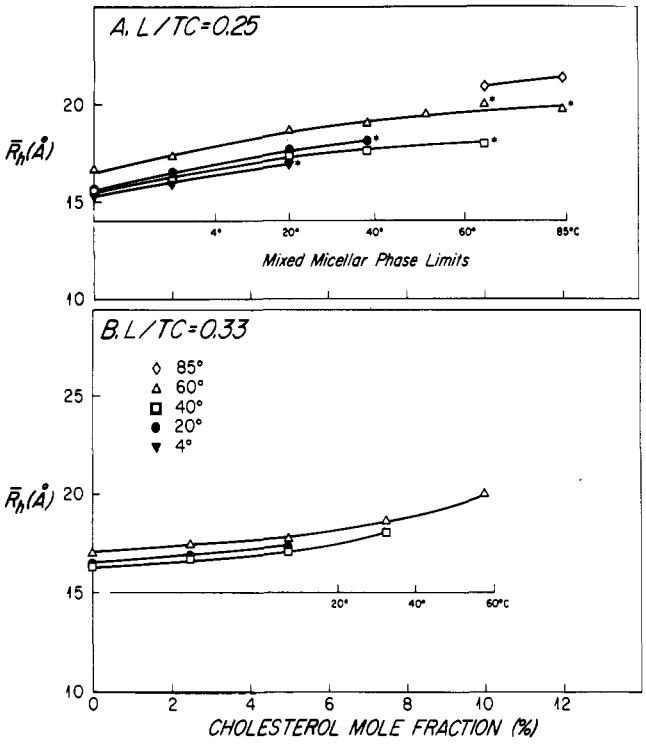

FIGURE 3: Mean hydrodynamic radius, $\bar{R}_h$ (angstroms), plotted as a function of the cholesterol mole fraction (percent) in concentrated (10 g/dL) type 2 systems at various temperatures. L/TC ratio is 0.25 in (A) and 0.33 in (B). Asterisks indicate metastably supersaturated systems whose cholesterol content exceeds the micellar phase limit.

total lipids, respectively. In 10 g/dL solutions, the $\bar{R}_h$ values measured at four different temperatures (5, 20, 40, and 60 °C) show a small but significant increase from ~10 to ~12 Å as X_{Ch} increases from 0 to 4%. No abrupt changes in $\bar{R}_h$ were noted in metastable solutions that had been supercooled from higher temperatures. The V values in all solutions remained at ~30%. In contrast, the 3 g/dL mixtures (Figure 2B) could not be appreciably supercooled, and thus the supersaturated systems contained two phases: a saturated micellar phase and a cholesterol crystalline precipitate. $\bar{R}_h$ measurements at 20 °C on the unsaturated systems (X_{Ch} < 1.1%) and on the supernatant phases at X_{Ch} = 2.5% and 5% showed only a slight increase of ~1 Å with added cholesterol.[2]

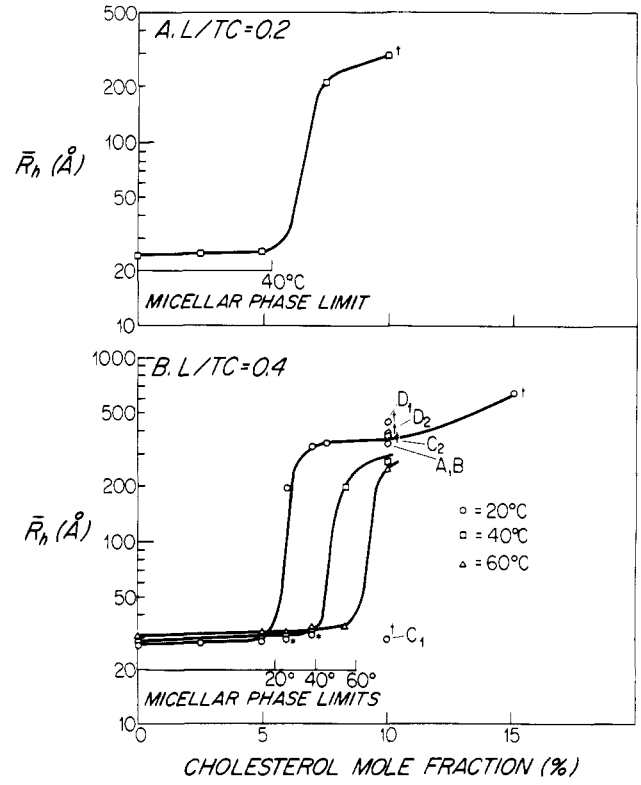

FIGURE 4: Mean hydrodynamic radii, $\bar{R}_h$ (angstroms), plotted as a function of the cholesterol mole fraction (percent) in dilute (3 g/dL) type 2 systems at various temperatures. L/TC ratio is 0.2 in (A) and 0.4 in (B). Asterisks indicate metastable supersaturated systems. Daggers indicate two-phase systems in which $\bar{R}_h$ corresponds to the supernatant phase. Samples prepared by different methods are indicated by the letters A, B, C_1, C_2, D_1, and D_2. See text for details.

Also shown in Figure 2A,B are dashed curves representing predictions of $\bar{R}_h$ on the basis of Woodford's model (Woodford, 1969) of bile salt–cholesterol solubilization. This model is not supported by the present data (see Discussion).

(2) Type 2 Systems: Ch Solubilization in Coexisting TC and Mixed TC–L Micelles. In Figures 3A,B and 4A,B, the dependence of $\bar{R}_h$ on X_{Ch} is shown for type 2 solutions at 10 and 3 g/dL, respectively.[3] In concentrated system, the $\bar{R}_h$ values measured at L/TC = 0.25 (Figure 3A) and 0.33 (Figure 3B) initially range from 15 to 17 Å and show a small increase of 2–3 Å as X_{Ch} varies from 0 to 12%, including metastable supersaturated solutions.[4] In the dilute solutions, $\bar{R}_h$ values measured at L/TC ratios of 0.2 (Figure 4A) and 0.4 (Figure 4B) start from 25–28 Å and also show a small increase of 1–2 Å with added cholesterol over the range where $X_{Ch} < X_{Ch}^{max}$. Above the phase limits, the dilute samples can also be supercooled to a limited extent (see Figure 4B), but after a period of hours, "stable" microprecipitates with $\bar{R}_h$ values in the 200–400 Å range are formed [see section B, (2), under Results]. In both concentrated and dilute micellar solutions, the V values were constant (40 ± 5%), consistent with the coexistence of the simple TC and mixed TC–L micelles (Mazer et al., 1980).

[2] The somewhat smaller $\bar{R}_h$ values obtained in 10 g/dL as compared to 3 g/dL systems reflect the influence of micellar interactions at the higher concentration, rather than an actual decrease in size (Mazer et al., 1979; Carey et al., 1981).

[3] These $\bar{R}_h$ values reflect the coexistence of simple TC micelles ($\bar{R}_s \simeq$ 10 Å) and mixed TC–L micelles ($\bar{R}_m \simeq$ 18 Å in 10 g/dL systems and 27 Å in 3 g/dL systems) as analyzed in Mazer et al. (1980).

[4] Similar QLS results have been reported by Oh et al. (1977) concerning the weak effect of solubilized cholesterol on the size of mixed BS–L micelles.

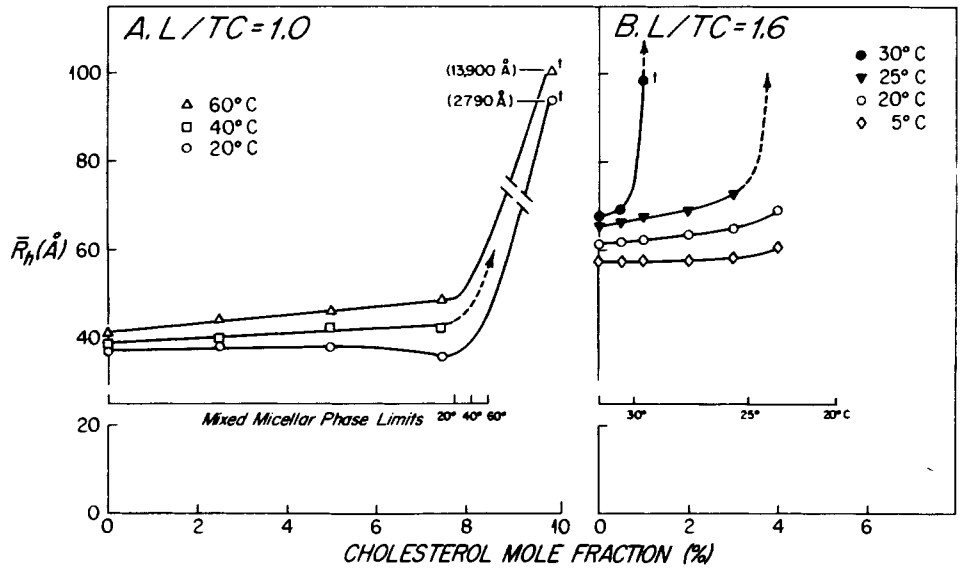

FIGURE 5: Mean hydrodynamic radii, $\bar{R}_h$ (angstroms), plotted as a function of the cholesterol mole fraction (percent) in concentrated (10 g/dL) type 3 systems at various temperatures. L/TC ratio is 1.0 in (A) and 1.6 in (B). Daggers denote supersaturated systems with two phases (micellar plus liquid crystalline).

(3) Type 3 Systems: Ch Solubilization in "Mixed Disc" TC–L Micelles. The dependence of $\bar{R}_h$ on X_{Ch} for type 3 mixtures at 10 and 3 g/dL is shown in Figures 5A,B and 6A,B, respectively. At L/TC ratios of 1.0 and 1.6, the $\bar{R}_h$ values in 10 g/dL solutions vary weakly with added Ch until the phase limits are reached (Figure 5A,B). Above this point, the $\bar{R}_h$ values abruptly increase, and the solutions become turbid and phase separate. Elevations in temperature influence this behavior by decreasing the X_{Ch}^{max} values where $\bar{R}_h$ grows abruptly (Figure 5B), the opposite of the temperature effect in type 2 systems (see Figure 1A). The polydispersity of these solutions was again independent of X_{Ch}, with V values of ~55% consistent with the properties of the "mixed disc" micelles in the absence of cholesterol (Mazer et al., 1980).

In the 3 g/dL systems, similar behavior was observed. At an L/TC ratio of 1.0 and temperature of 20 °C (Figure 6A), $\bar{R}_h$ is initially 70 Å and varies weakly with X_{Ch} below the phase limit ($X_{Ch}^{max} \simeq 8\%$). At 40 °C, the $\bar{R}_h$ values are about 10 Å larger and parallel the behavior at 20 °C. Above the phase limits, $\bar{R}_h$ increases to the 600–800-Å size range, but the solutions do not spontaneously phase separate (as occurred in the corresponding 10 g/dL systems). Additional experimental evidence suggests that the large particles formed in these dilute supersaturated systems are unilamellar vesicles [see section B, (3), under Results]. The $\bar{R}_h$ values measured at an L/TC ratio of 1.2 [close to the bile salt–lecithin solubilization limit (Figure 1B)] behave similarly (Figure 6B) to that in Figure 6A. Below the phase limit ($X_{Ch}^{max} \simeq 4\%$), the influence of added cholesterol on the large "mixed disc" micelles ($\bar{R}_h \simeq$ 120 Å) is small. Above the phase limit, the solutions are macroscopically turbid but do not phase separate under gravity. QLS measurements performed prior to centrifugation showed very large particles ($\bar{R}_h \simeq$ 1500 Å). Centrifugation (10000*g* for 30 min) resulted in an optically clear supernatant phase whose $\bar{R}_h$ value was ~100 Å, comparable to the sizes of the "mixed disc" micelles formed below the phase limit. These findings suggest that the type 3 micellar phase does, in fact, coexist with the large vesicle structures [see section B, (3), under Results]. The V values of the dilute type 3 systems below the phase limit were comparable to those in the 10 g/dL solutions.

(B) Supersaturated Systems: Size, Kinetics, and Composition of Microprecipitates. We have utilized the strong

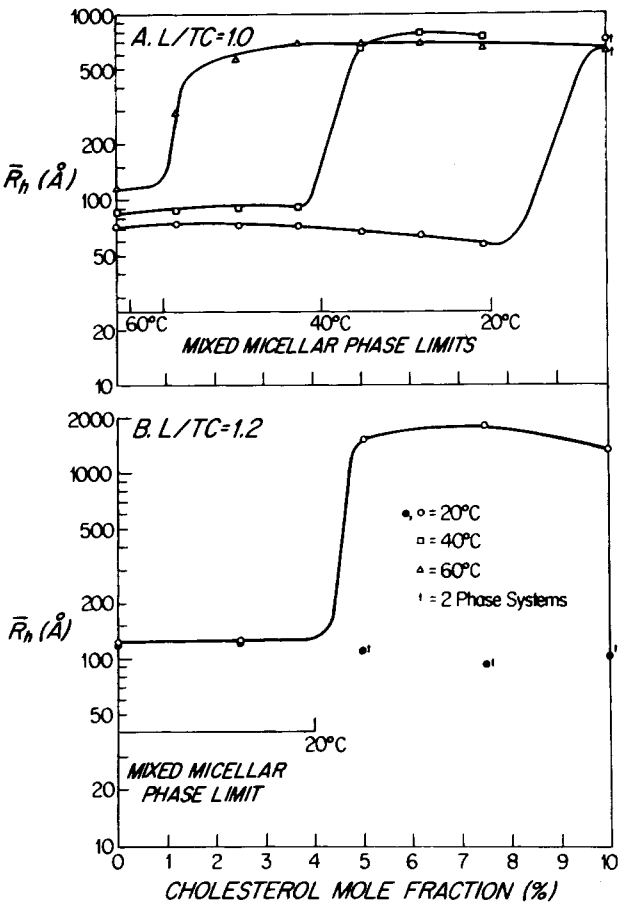

FIGURE 6: Mean hydrodynamic radii, $\bar{R}_h$ (angstroms), plotted as a function of the cholesterol mole fraction (percent) in dilute (3 g/dL) type 3 systems at various temperatures. L/TC ratio is 1.0 in (A) and 1.2 in (B). Daggers indicates two-phase systems in which $\bar{R}_h$ values correspond to the supernatant phase. In (B), open and closed circles denote samples studied before and after centrifugation (10000*g* for 20 min), respectively.

temperature dependence of the cholesterol solubilization limit, $X_{Ch}^{max}(T)$ (Carey & Small, 1978), as a means for varying the cholesterol saturation ratio, S [defined as $X_{Ch}/[X_{Ch}^{max}(T)]$] from a value less than unity (unsaturated) at the temperature T_i to a value exceeding unity (supersaturated) at the tem-

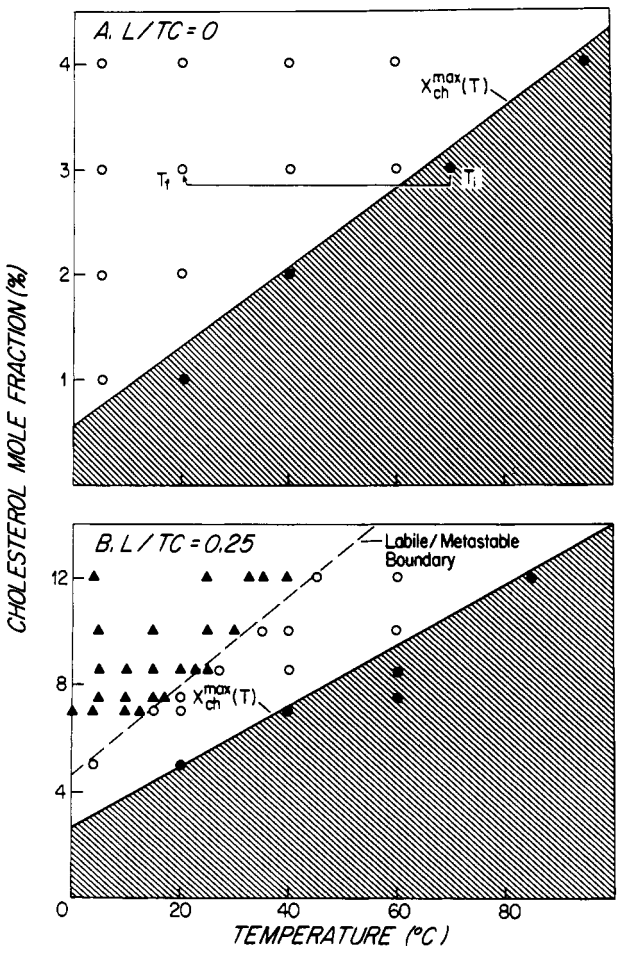

FIGURE 7: Temperature dependence of the cholesterol solubilization limits, $X_{Ch}^{max}(T)$, in 10 g/dL type 1 systems in (A) and type 2 systems (L/TC = 0.25) in (B). Also indicated is the precipitation behavior of supersaturated systems studied by the temperature change ($T_i \rightarrow T_f$) (see text for details). At T_i closed circles correspond to unsaturated systems. At T_f, open circles denote metastable systems, and triangles denote labile precipitating systems. The broken line denotes the metastable/labile boundary.

perature T_f (see Methods). At the final temperature, T_f, scattered intensity measurements were made to characterize the nucleation kinetics of microprecipitation, and QLS measurements of $\bar{R}_h$ and V were obtained to characterize the size distribution of the microprecipitates. The TEM appearance, sedimentation behavior, and biliary lipid compositions of the precipitate phases are also reported. In the case of the 3 g/dL type 2 systems, we further examined the formation of microprecipitates as a function of the path by which the composition and temperature of the supersaturated system were established.

(1) Supersaturated Bile Salt–Cholesterol (Type 1) Systems. The temperature dependence of $X_{Ch}^{max}(T)$ for 10 g/dL type 1 systems (L/TC = 0) as derived from the solubilization studies of Carey & Small (1978) is plotted in Figure 7A. Temperature change experiments ($T_i \rightarrow T_f$) are indicated on this figure as horizontal jumps from points in the shaded area (T_i) to points in the unshaded area (T_f), where cholesterol monohydrate precipitates are known to form at equilibrium (Admirand & Small, 1968; Holzbach et al., 1973; Carey & Small, 1978). For all the supersaturated systems studied in Figure 7A, measurements of the scattered light intensity showed no detectable changes after 1 h at the temperature T_f, indicating ~a metastable state (open circles). This was found even at the highest supersaturation ratio, S = 5.3, corresponding to X_{Ch} = 4%, T_i = 85 °C, and T_f = 5 °C. However, by ~48 h, macroscopic cholesterol crystals had precipitated in many of the supersaturated systems. In the case of the dilute type 1 systems, the weaker temperature dependence of the cholesterol solubilization limit X_{Ch}^{max} (M. C. Carey and D. M. Small, unpublished experiments) made it impossible to create appreciable degrees of supersaturation by varying the temperature. As a result, the metastability of these systems could not be determined.

(2) Microprecipitation in Type 2 "Coexistence" Systems. (a) 10 g/dL Systems. In Figure 7B, the temperature dependence of $X_{Ch}^{max}(T)$ has been plotted for 10 g/dL type 2 systems (L/TC = 0.25) as derived from Carey & Small (1978). At this L/TC ratio, the equilibrium precipitate phase formed above the phase boundary is also cholesterol monohydrate (Carey & Small, 1978). However, prior to the formation of the equilibrium precipitate, Holzbach and coworkers (Holzbach et al., 1976; Holzbach & Corbusier, 1978) have shown that a nonequilibrium liquid-crystalline phase forms transiently in these systems. By use of the temperature change method ($T_i \rightarrow T_f$), we have studied the initial stages of microprecipitation in the type 2 systems as a function of the degree of supersaturation S. The qualitative results are shown in Figure 7B and are represented by two symbols. The open circles indicate metastable systems which behaved similarly to the supersaturated type 1 systems. The solid triangles denote "labile" systems in which microprecipitation occurred in less than 1 h. The S ratio corresponding to the boundary between labile and metastable systems (dashed line) was found to be approximately 1.6 at all temperatures.

Figure 8 displays examples of the microprecipitation kinetics from labile systems as monitored by the time dependence of the scattered light intensity, $\bar{I}(t)/[\bar{I}(0)]$. The systems shown

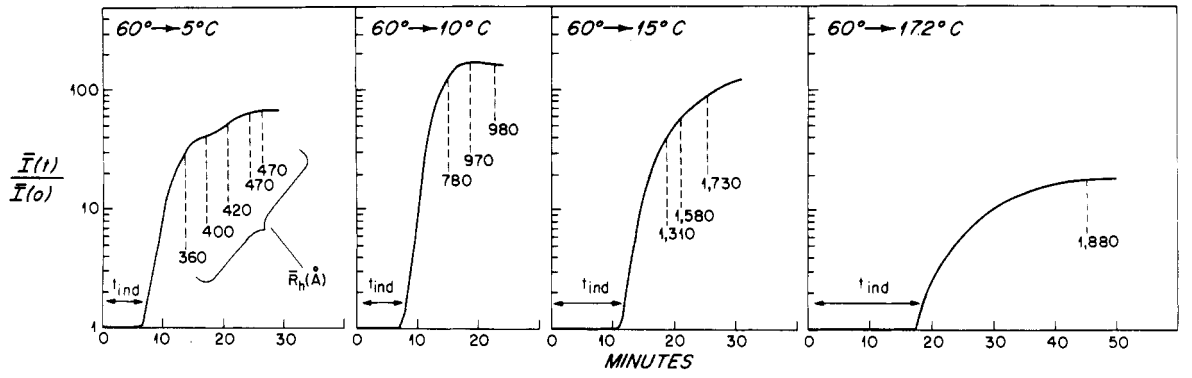

FIGURE 8: Time dependence of scattered light intensity, $\bar{I}(t)/[\bar{I}(0)]$, resulting from temperature change experiments conducted on a 10 g/dL sample containing L/TC = 0.25 and X_{Ch} = 7.5%. t_{ind} denotes the induction time which precedes any detectable microprecipitation. Also indicated are $\bar{R}_h$ values (in angstroms) corresponding to the sizes of the microprecipitates.

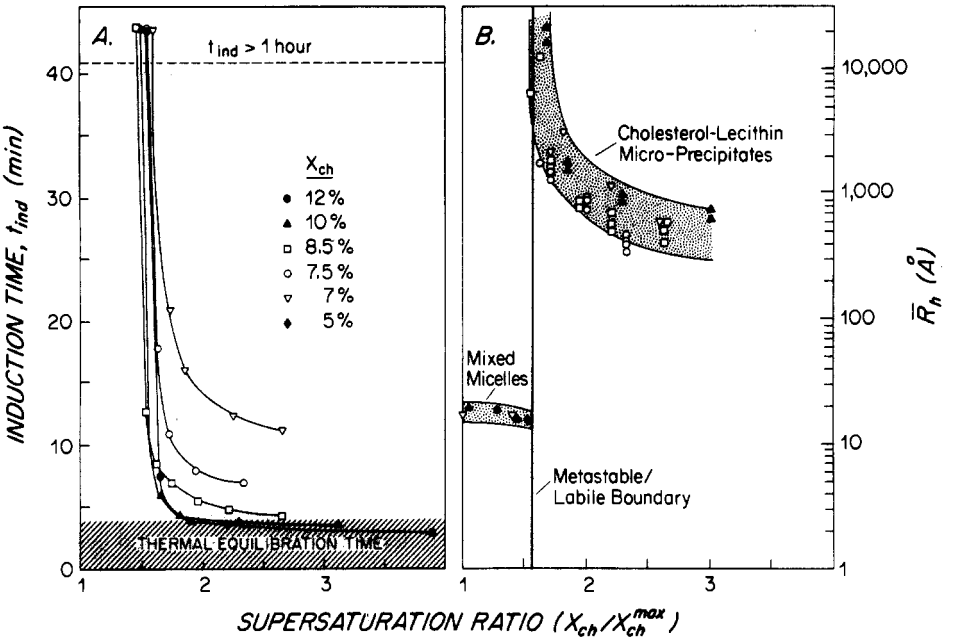

FIGURE 9: Induction time (t_{ind}) and mean hydrodynamic radii, $\bar{R}_h$, of microprecipitates corresponding to labile type 2 systems. In (A), t_{ind} is plotted as a function of the supersaturation ratio (S) for systems with different cholesterol mole fractions (X_{Ch}). The shaded area indicates the thermal equilibration time for making temperature changes ($T_i \rightarrow T_f$). In (B), $\bar{R}_h$ is plotted vs. S for the same systems. Both quantities increase dramatically, as S approaches the metastable/labile limit of ~1.6. Below this limit, the $\bar{R}_h$ values of metastable mixed micellar systems are shown in (B).

all have the same X_{Ch} = 7.5% and T_i = 60 °C but have been cooled to different T_f values, 5, 10, 15, and 17.2 °C. In each case, $\bar{I}(t)/[\bar{I}(0)]$ initially showed no detectable change for a period of time ranging from 7 to 18 min. This period exceeds the thermal equilibration time needed to make the temperature change (~4 min) and represents an induction time (denoted t_{ind}) for nucleation (Walton, 1967). Once t_{ind} was reached, a rapid increase in $\bar{I}(t)/[\bar{I}(0)]$ occurred, marking the onset of detectable microprecipitation. Thereafter, $\bar{I}(t)/[\bar{I}(0)]$ varied slowly, and QLS measurements of $\bar{R}_h$ were made. Under these conditions, the scattering by micelles is negligible, and thus, $\bar{R}_h$ corresponds to the distribution of microprecipitates. The final sizes of the microprecipitates ranged from 470 to 1880 Å, varying inversely with the magnitude of the temperature change. The general features shown in Figure 8 are typical of the behavior found for all labile systems represented in Figure 7B (Mazer, 1978), when analyzed in terms of the corresponding supersaturation ratios. As seen in panels A and B of Figure 9, both the induction times and the microprecipitate sizes, respectively, in all systems increase dramatically as the supersaturation ratio decreases from high values ($S \simeq 4.0$) and approaches the metastable/labile limit ($S \simeq 1.6$). Such behavior is typical of a homogeneous nucleation process (Walton, 1967) as will be discussed later. The V values of the microprecipitates ranged from 30 to 60% and displayed no systematic variation with $\bar{R}_h$ or S.

Transmission electron photomicrographs of the microprecipitates formed in a 10 g/dL system (Figure 1A) show numerous dark ("positively" stained) spherical particles with radii (500–2500 Å) which are comparable in size to the $\bar{R}_h$ values measured by QLS (1570–1880 Å). It is evident that these globular particles do not resemble cholesterol monohydrate crystals (Jandacek et al., 1977) but are similar (although much smaller) to the liquid-crystalline droplets reported by Holzbach & Marsh (1975) in analogous model bile systems.

Centrifugation of labile supersaturated systems [see section C, (3), under Experimental Procedures] separated the microprecipitates into a phase of lower density than the infranatant micellar solution ($\rho \simeq 1.02$ g/mL, 20 °C), further suggesting that the precipitates differ from cholesterol monohydrate or anhydrate whose densities are 1.03 and 1.05 g/mL, respectively (Gershfeld, 1978). Biliary lipid analyses of the stock solutions, infranatant phases, and isolated precipitate phases are shown in Table I. The stock solutions show a variation in the cholesterol mole fraction and constancy in the L/TC molar ratios (0.275 ± 0.005) that are in good agreement with the desired compositions. The differences in cholesterol contents between stock and infranatant solutions are quantitatively accounted for by the amount of cholesterol found in the precipitate phases. The amounts of lecithin (mole fraction ≃ 28%) and TC (mole fraction ≃ 30%) found in the precipitates are considerable. That these amounts reflect more than just contamination of the precipitate with a residual amount of infranatant solution is evident from the fact that the L/TC ratio of the precipitates (0.9 ± 0.2 is significantly greater than the L/TC ratio of the micellar phases (0.275 ± 0.005). A lower limit for the "true" lecithin content of the precipitates was estimated by assuming that the bile salt content in the precipitate is due entirely to contamination by the infranatant micellar phase.[5] The "corrected" precipitate values (Table I) show that for all four samples, the cholesterol/lecithin mole ratio is approximately 2/1, independent of the amount of cholesterol precipitated.

(*b*) *3 g/dL Systems.* As shown in Figure 4, the dilute type 2 systems (L/TC = 0.2 and 0.4) contain stable microprecipitates ($\bar{R}_h$ = 200–400 Å) when X_{Ch} exceeds the phase limit X_{Ch}^{max}. The polydispersity of these systems is small ($V \simeq$ 20–30%) at X_{Ch} values well above the phase limit. However, close to X_{Ch}^{max}, V is large (~100%), reflecting the total polydispersity of both micelles and microprecipitates. The dilute

[5] Calculations show that the observed bile salt content of the precipitates would result from contamination with as little as 20 μL of infranatant from the original 0.5 mL of sample. This infranatant solution would likewise contribute small amounts of lecithin and cholesterol which have been subtracted in the "corrected" precipitate values of Table I.

Table I: Biliary Lipid Analyses of 10 g/dL Type 2 Systems

	7.5%[a]			8.5%			10%			12%		
	TC	L	Ch	TC	L	Ch	TC	L	Ch	TC	L	Ch
stock solutions												
mg/0.5 mL	32.3	13.3	2.5	33.1	13.3	3.0	33.1	13.1	3.4	33.9	13.3	4.2
mole fraction (%)	71.8	20.4	7.8	71.4	19.8	8.8	70.16	19.4	10.0	69.3	18.8	11.9
L/TC molar ratio		0.28			0.28			0.27			0.27	0.275 ± 0.005[b]
infranatants												
mg/0.5 mL	31.5	12.6	1.9	31.7	13.1	2.0	33.2	12.5	1.9	30.7	12.5	2.0
mole fraction (%)	73.5	20.4	6.1	72.8	20.9	6.3	73.9	19.9	6.2	72.8	20.6	6.6
L/TC molar ratio		0.28			0.29			0.27			0.28	0.28 ± 0.008[b]
Ch/L molar ratio		0.30			0.30			0.31			0.32	0.31 ± 0.01[b]
precipitates (uncorr)												
mg/0.5 mL	0.8	0.8	0.6	1.3	1.3	0.7	1.5	1.9	1.5	1.5	2.5	2.0
mole fraction (%)	37.2	26.4	36.4	40.4	27.7	31.9	29.9	27.2	42.9	24.5	29.3	46.2
L/TC molar ratio		0.71			0.69			0.91			1.2	0.9 ± 0.2[b]
Ch/L molar ratio		1.38			1.15			1.58			1.58	1.40 ± 0.2[b]
precipitates (corr)												
mg/0.5 mL		0.48	0.55		0.76	0.62		1.32	1.41		1.89	1.90
mole fraction (%)		30	70		38	62		31.9	68.1		33.2	66.8
Ch/L molar ratio		2.3			1.6			2.1			2.0	2.0 ± 0.3[b]

[a] Percentages represent desired mole fraction of cholesterol in original mixtures. [b] Average of the four samples ± SEM.

systems with L/TC = 0.4 remain as stable microdispersions even under high-speed ultracentrifugation (240000*g* for 25 h) except at very high X_{Ch} values (12–15%). This apparent stability of the "dilute microprecipitates" as a macroscopic "single phase" is distinct from the behavior of the 10 g/dL labile systems and also from the true metastability of the micellar phases which are seen in both 10 and 3 g/dL systems (Figures 3A and 4B).

Visualization of the microprecipitates by TEM (Figure 11B) shows globular microdroplets with radii of 300–500 Å comparable to the sizes and polydispersity obtained by QLS. From the sedimentation properties of these microdroplets, it can be deduced that their density is nearly equal[6] to that of the 3 g/dL type 2 micellar solution ($\rho \simeq 1.008$ g/mL), consistent with the presence of both lecithin and cholesterol. By changing the density of the micellar solution with D_2O, we isolated these particles by high-speed ultracentrifugation (see Experimental Procedures). Upon analysis, the resulting Ch/L molar ratio was 0.9 ± 0.1 (uncorrected) and 2.1 ± 0.5 (corrected),[7] comparable to the ratios found for the separated precipitates in the 10 g/dL systems (Table I).

Insights into the thermodynamic aspects of the microdroplet formation were obtained by preparing identical samples (L/TC = 0.4, X_{Ch} = 10%, T = 20 °C) by using different "paths" (see Experimental Procedures). As shown in Figure 4B, the coprecipitation method (path A) and dilution method (path B) both yield "single phase" systems containing microdroplets with $\bar{R}_h \simeq 350$ Å. In contrast, path C1, in which cholesterol monohydrate crystals are equilibrated with a TC–L micellar solution at 20 °C, remains as a two-phase system containing saturated micelles ($\bar{R}_h \simeq 30$ Å) and precipitated crystals. When the same system was incubated at 90 °C for 3 h and then cooled to 20 °C (path C2), microdroplets with an $\bar{R}_h$ of ~380 Å were formed (Figure 4B). Finally, in paths D_1 and D_2, the interaction of TC solutions with lecithin–cholesterol lamellar dispersions shows that in the supernatant phases of both systems, microdroplets were formed with $\bar{R}_h$ values of 400 and 450 Å, respectively.

(*3*) *Supersaturation in "Mixed Disc" (Type 3) Micellar Systems.* As seen in Figure 5A,B, the supersaturated 10 g/dL systems contain very large aggregates ($\bar{R}_h > 3000$ Å) which ultimately form a separate macroscopic phase. This behavior occurs either by a "path A" method of sample preparation (Figure 5A) or by elevating the sample temperature (Figure 5B). From the studies of Carey & Small (1978), these precipitated phases correspond to an equilibrium liquid-crystalline structure containing both lecithin and cholesterol.

In the 3 g/dL mixtures (Figure 6A,B), a similar phenomenon occurs in the supersaturated systems; however, the aggregates remain microscopic and do not spontaneously phase separate. For an L/TC ratio of 1.0 (Figure 6A), $\bar{R}_h$ values at high cholesterol supersaturations approached 600–800 Å at 20, 40, and 60 °C. The polydispersity associated with these stable microprecipitates was small ($V \simeq$ 10–25%). Just above the phase boundary, however, the scattering of light by the saturated micellar phase is comparable to that of the microprecipitates and results in a smaller $\bar{R}_h$ for the entire system (~300 Å) and a substantial increase in polydispersity $V \simeq$ 120% (Figure 6A, T = 60 °C). Biliary lipid analyses on two centrifuged systems (L/TC = 1.2, X_{Ch} = 7.5 and 10%, T = 20 °C) revealed that the type 3 precipitated phases consist predominantly of lecithin in a 4:1 ratio with cholesterol, and under polarized light microscopy, myelin figures were seen, indicative of a lamellar liquid-crystalline structure. In view of these findings, the stable microprecipitates in dilute type 3 systems are most likely unilamellar vesicles. Further evidence for this view derives from light-scattering dissymmetry measurements which showed the mean radius of gyration, $\bar{R}_g$, of the particles to be nearly equal to $\bar{R}_h$ for the relatively monodisperse supersaturated type 3 systems (Mazer, 1978). The near identity of the two size parameters would be expected if the microprecipitates are large single shelled (unilamellar) vesicles,[8] and would exclude rod-shaped or solid spherical

[6] This deduction is based on the observation that ultracentrifugation at 240000*g* for 25 h did not sediment the "stable" microdroplets from solution. Using the Svedberg equation (Moore, 1972) in combination with the measured diffusion coefficient ($\bar{D}_{20°C} = 5.35 \times 10^{-8}$ cm^2/s), estimated molecular mass (~1.6×10^8 g/mol), and centrifuge tube dimensions (~2 cm), we calculate that the buoyancy factor ($1 - \bar{v}\rho$) is less than 5×10^{-4}.

[7] The "correction" is for possible contamination of the microdroplet phase with the infranatant micellar solution as done in Table I.

[8] $\bar{R}_h$ and $\bar{R}_g$ will be nearly the same for monodisperse spherical shells when the bilayer thickness (t) is small compared to the outer radius of the shell (R). In the case of lecithin–cholesterol vesicles, $t \simeq 55$ Å (Newman & Huang, 1975) is far smaller than R = 600–800 Å found in the type 3 systems.

particles (Young et al., 1978). Recent studies using freeze–fracture electron microscopy (EM) (P. Schurtenberger et al., unpublished experiments) confirm the presence of unilamellar vesicles in very dilute (<1 g/dL) bile salt–lecithin systems where $\bar{R}_g$ is also found to nearly equal $\bar{R}_h$.

Discussion

(*A*) *Molecular Aspects of Cholesterol Solubilization and Precipitation—An Overview.* The present studies, taken together with our previous QLS investigations (Mazer et al., 1979, 1980; Carey et al., 1981) and the available phase equilibria information on biliary lipid systems (Carey & Small, 1978; Holzbach & Marsh, 1975; Holzbach et al., 1976; Holzbach & Corbusier, 1978), permit the development of a conceptual picture of cholesterol solubilization and precipitation in model bile. Figure 11 displays a highly schematized presentation of these concepts for type 1 and type 2 systems (panel A) and type 3 systems (panel B). For unsaturated systems, we have suggested that cholesterol monomers can bind to the various micellar species (i.e., simple TC micelles, small TC–L micelles, and large "mixed disc" micelles) without significantly perturbing the preexisting structures or micellization equilibria. Such binding reflects an equilibrium between free and bound cholesterol molecules and provides insight into the origin of the solubilization limits and the coexistence of precipitated phases. To understand these phenomena, it must be recognized that as the cholesterol binding increases, so too does the concentration of free cholesterol monomers in solution (i.e., the chemical potential of cholesterol in the system increases). However, as more cholesterol is solubilized, the free concentration will eventually approach and exceed its solubility in the monomer state. This occurs when the chemical potential of cholesterol in the system reaches and exceeds the value corresponding to the chemical potential of the precipitate phase (Walton, 1967). Under such conditions, the micellar phase is supersaturated by virtue of the excess monomer concentration and at equilibrium will consist of micelles, a coexisting precipitate phase, and a cholesterol monomer concentration equal to the solubility limit.[9] For type 1 and 2 systems of the common bile salts, the equilibrium precipitate phase is known to be cholesterol monohydrate (Carey & Small, 1978) as indicated in Figure 11A, whereas in type 3 systems, the equilibrium precipitate is a liquid-crystalline lamellar phase containing lecithin and cholesterol (Holzbach & Marsh, 1975; Carey & Small, 1978). This lamellar phase coalesces and phase separates in concentrated (10 g/dL) systems but can remain dispersed in a microscopic vesicle state in dilute (3 g/dL) systems (Figure 11B), a new finding which has not been reported previously. Our present studies also confirm the formation of nonequilibrium coprecipitate phases in the labile type 2 systems, as previously noted by Holzbach and co-workers (Holzbach & Marsh, 1975; Holzbach et al., 1976; Holzbach & Corbusier, 1978). These phases are found to contain cholesterol and lecithin in a molar ratio of approximately 2 to 1, similar to the findings of Holzbach & Corbusier (1978), and are apparently cholesterol-rich liquid crystals. Although the microstructure of this nonequilibrium phase is unknown, we propose in Figure 11A a multilamellar droplet structure for the microprecipitates, consistent with our TEM studies (Figure 10A,B). In the dilute (3 g/dL) systems, these microdroplets remain as a stable dispersion in solution, whereas in the 10 g/dL systems, they ultimately coalesce and phase separate. Sequential observations of the coalesced liquid-crystalline phase, by Holzbach & Corbusier (1978), indicate a conversion into solid cholesterol crystals occurring by about 20 days, consistent with the "equilibrium" observations of Carey and Small made at 30 days. This conversion is indicated in Figure 11A, thus completing the path from the supersaturated micellar phase through the liquid-crystalline phase to cholesterol monohydrate.[10]

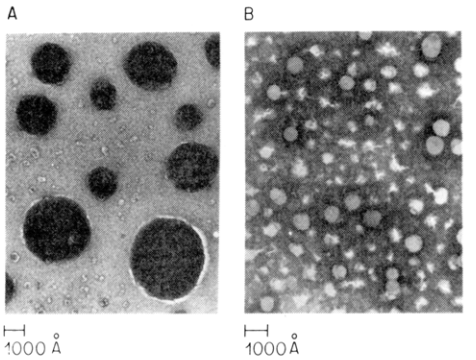

FIGURE 10: Transmission electron micrographs of microprecipitates. Plate A corresponds to microprecipitates formed in 10 g/dL labile type 2 systems that were stained with 1% phosphotungstic acid. Plate B corresponds to microprecipitates formed in 3 g/dL type 2 systems that were stained with 1% uranyl acetate. In both cases, particles appear to be spherical droplets with radii comparable to $\bar{R}_h$ values obtained by QLS (see text and Experimental Procedures for details).

(*B*) *Quantitative Aspects of Cholesterol Solubilization.* The concepts of cholesterol binding depicted in Figure 11 will now be applied to a quantitative analysis of cholesterol solubilization in model bile solutions. Derivations of some of the mathematical equations are presented under Appendix A.

(*1*) *Type 1 Systems: Cholesterol Binding to Simple Bile Salt Micelles.* Our findings (Figure 2) that cholesterol molecules bind to simple taurocholate micelles without significantly altering the micellar structure are supported by the studies of Feldman & Borgström (1966) and Small (1971). In contrast, Woodford's model of cholesterol solubilization (Woodford, 1969) proposes the formation of large bile salt–cholesterol micelles ($\bar{R}_h$ = 16.3 Å) containing 25 bile salts and 1 cholesterol, but as shown in Figure 2A,B, the experimental $\bar{R}_h$ values are not consistent with the predictions of the Woodford (1969) model.[11] We therefore assume in our analysis of type 1 systems that each taurocholate micelle, which contains four to eight bile salts (Mazer et al., 1979; Small, 1968; Vitello, 1971), possesses a single binding site for cholesterol solubilization. This implies that the ratio of binding sites to micellized bile salts, a parameter denoted as α_1 in our theory, is approximately 0.2 for the TC–Ch system. Although it is not known precisely where the cholesterol binding site is located in the micelle, we have recently suggested (Carey et al., 1981) that hydrophobic bonding of the monomer to the outer surface of the micelle may in fact be the thermodynamic driving force for cholesterol solubilization by all bile salt species. Such details, however, are not vital for our analysis and are implicitly contained in the cholesterol binding constant, $K_1(T)$, which is assumed to be temperature dependent. As

[9] The general concepts employed here are similar to the model of naphthalene solubilization in sodium cholate solutions proposed by Mukerjee & Cardinal (1976).

[10] Accumulating evidence (Corrigan et al., 1980; Salvioli et al., 1981) suggests that this path may be partially reversible (i.e., cholesterol monohydrate → liquid-crystalline phase) in biliary lipid solutions containing conjugated ursodeoxycholate.

[11] This discrepancy may be due to problems of microbial contamination cited in Woodford's experimental studies.

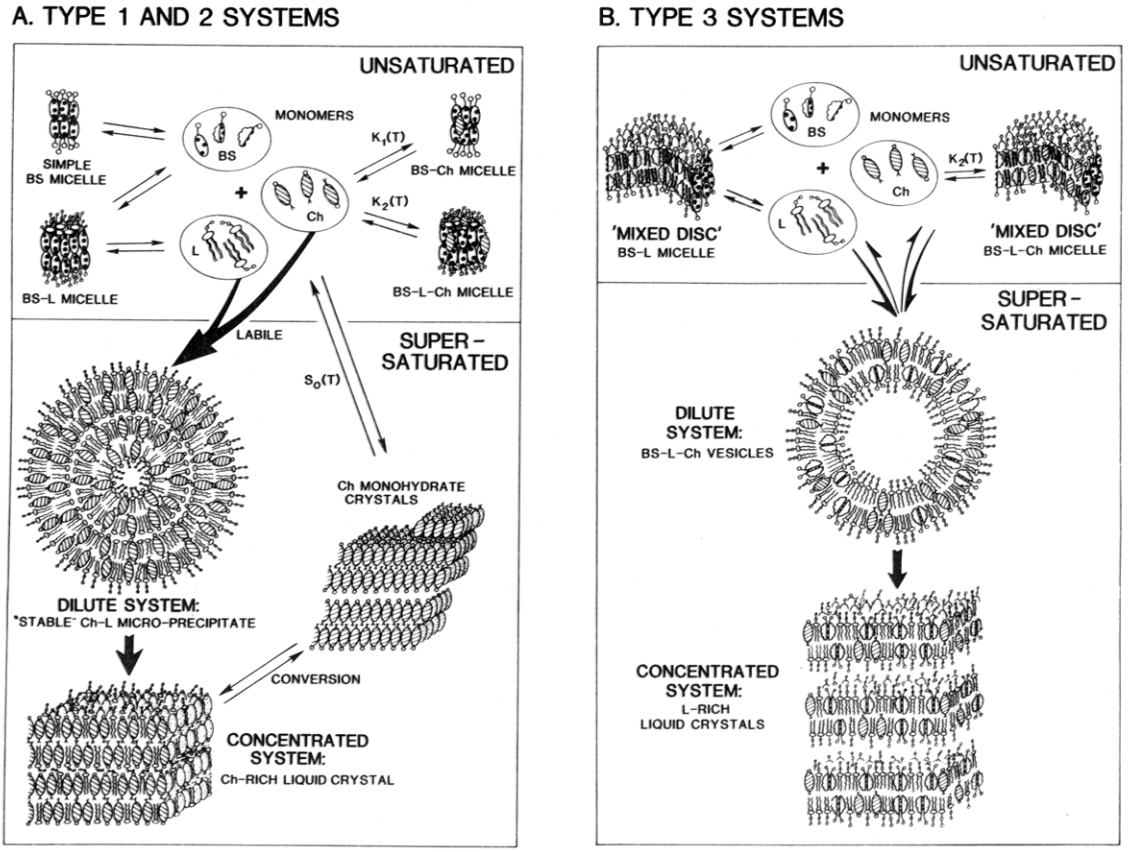

FIGURE 11: Schematic diagram of cholesterol solubilization and precipitation in type 1 and 2 systems (A) and type 3 systems (B). The upper half of both panels depicts equilibria between bile salt (BS), lecithin (L), and cholesterol (Ch) monomers and micellar aggregates in unsaturated systems. The binding of cholesterol to simple BS micelles and coexisting mixed BS–L micelles (A) is characterized by the binding constants $K_1(T)$ and $K_2(T)$, respectively. Cholesterol binding to large "mixed disc" BS–L micelles (B) is also characterized by $K_2(T)$. In supersaturated systems (lower half of both panels), monomers interact to form precipitate phases. In type 1 and 2 systems, the equilibrium precipitate is cholesterol monohydrate; however, labile precipitating systems produce Ch–L microprecipitates initially. These remain stable in dilute type 2 systems but coalesce to form Ch-rich liquid crystals in concentrated systems and are subsequently converted to cholesterol monohydrate. In type 3 supersaturated systems, BS–L–Ch vesicles form in dilute systems but coalesce to form L-rich liquid crystals in concentrated systems. See text for additional details.

derived under Appendix A, the mole fractions of cholesterol, $X_{Ch}^{max}(T)$, corresponding to the solubilization limit in a concentrated (i.e., 10 g/dL) type 1 system will depend only on the parameters α_1 and $K_1(T)$ and on the monomeric solubility of cholesterol monohydrate, $S_0(T)$, according to

$$X_{Ch}^{max}(T) = \frac{A_1(T)}{1 + A_1(T)} \tag{1a}$$

where $A_1(T)$ is given by

$$A_1(T) = \alpha_1 \left[\frac{K_1(T)S_0(T)}{1 + K_1(T)S_0(T)} \right] \tag{1b}$$

Only in the limit when the product $K_1(T)S_0(T)$ greatly exceeds unity will the cholesterol binding sites become fully occupied. Under these conditions, $X_{Ch}^{max}(T)$ will approach $\alpha_1/(1 + \alpha_1)$. When $K_1(T)S_0(T)$ is less than unity, the binding sites will not be fully occupied at the solubilization limit, but as in the former case, the cholesterol monomer concentration will have reached the value $S_0(T)$, at which point an equilibrium with precipitated cholesterol monohydrate is established.

To evaluate the thermodynamic parameters of cholesterol solubilization in type 1 systems, we have used eq 1a,b to analyze the known temperature dependence of X_{Ch}^{max} for 10 g/dL TC–Ch systems (i.e., solid line in Figure 7A). Figure 12A illustrates our deductions of $A_1(T)$ and $K_1(T)S_0(T)$ plotted logarithmically on an inverse temperature scale (1/K). Both quantities are found to increase monotonically as functions of temperature, reflecting the behavior of $X_{Ch}^{max}(T)$. From the mean slope of the $K_1(T)S_0(T)$ curve, we have deduced the enthalpy difference ($H_{bound} - H_{ppt}$) for transferring a cholesterol molecule from the monohydrate precipitate to the TC micelle binding site and obtain a value of 18.3 kJ/mol (see Appendix A, eq A-9). This implies a large *unfavorable* (endothermic) enthalpy change for cholesterol monohydrate solubilization whose physical significance will be discussed later. Further insight into the thermodynamics of cholesterol solubilization has come from estimating the magnitude of $K_1(T)$. Using the $S_0(T)$ value of Saad & Higuchi (1965) at 30 °C, 6.7×10^{-8} M, we have deduced from the product $K_1(T)S_0(T)$ that K_1(30 °C) equals 1.3×10^6 L/mol. This implies that the unitary free-energy change for transferring cholesterol from the monomeric state to the TC micelle is –45.1 kJ/mol a value comparable to that found for cholesterol binding to $NaDodSO_4$ micelles (Gilbert & Reynolds, 1976) and also consistent with the thermodynamics of hydrophobic bonding (Carey et al., 1981). Despite this favorable free-energy change, the overall transfer from monohydrate precipitate to micelle is unfavorable, +6.21 kJ/mol, as deduced from the product K(30 °C)S_1(30 °C) = 0.085 (see Appendix A, eq A-8). This implies that the percent occupancy of all potential binding sites on the TC micelles is less than 10% when the solubilization limit is reached.

(*2*) *Type 2 Systems: Cholesterol Binding to Coexisting Simple and Mixed Micelles.* To extend our thermodynamic analysis to type 2 systems, it is necessary to characterize both

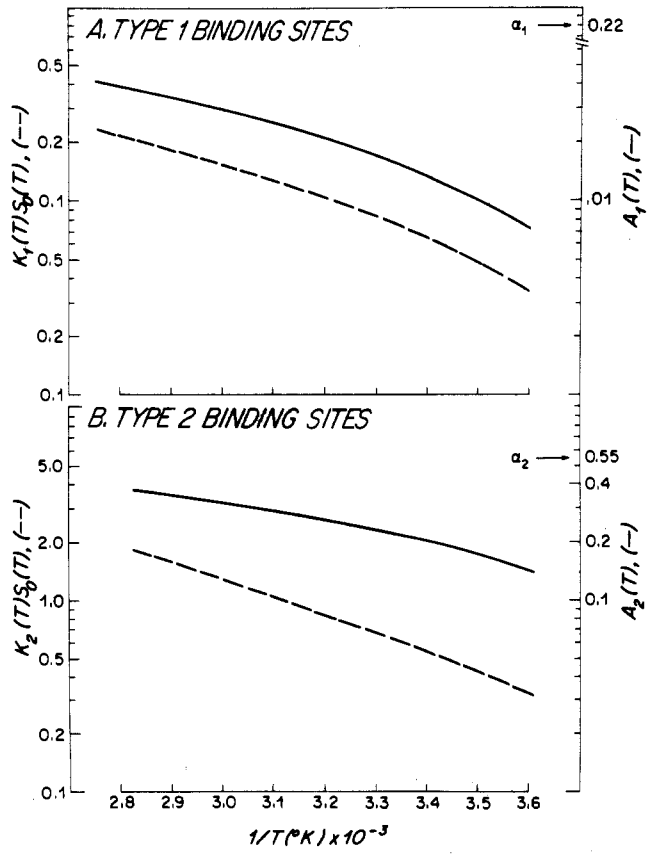

FIGURE 12: Temperature dependence of the cholesterol binding parameters for type 1 and 2 binding sites plotted vs. $1/T$ (T in kelvin). The simple TC micelle parameters $A_1(T)$ and $K_1(T)S_0(T)$ are plotted in (A). The mixed TC–L micelle parameters $A_2(T)$ and $K_2(T)S_0(T)$ are plotted in (B). Values of the parameters α_1 and α_2 employed in these deductions were 0.22 and 0.55, respectively. See text for explanation.

the number and affinity of cholesterol binding sites in the TC–L mixed micelles which form in these systems. For this purpose, we introduce the parameters α_2, the ratio of cholesterol binding sites to lecithin molecules in the mixed micelle, and $K_2(T)$, the binding affinity which is assumed to be temperature dependent. Using our previous quantitative description for the coexistence of simple and mixed micelles in type 2 systems (Mazer et al., 1980), it can be shown (see Appendix A for details) that the solubilization limit $X_{Ch}^{max}(T)$ in 10 g/dL type 2 systems will be a function of the L/BS ratio given by

$$X_{Ch}^{max}(T) = \frac{\left[1 - \gamma^{-1}\frac{[L]}{[BS]}\right]A_1(T) + \frac{[L]}{[BS]}A_2(T)}{1 + \frac{[L]}{[BS]} + \left[1 - \gamma^{-1}\frac{[L]}{[BS]}\right]A_1(T) + \frac{[L]}{[BS]}A_2(T)} \quad (2a)$$

where γ is the lecithin to bile salt ratio in the coexisting mixed micelle, $A_1(T)$ is the parameter defined in eq 1b, and $A_2(T)$ is the function of α_2, $K_2(T)$, and $S_0(T)$, defined by

$$A_2(T) = \alpha_2\left[\frac{K_2(T)S_0(T)}{1 + K_2(T)S_0(T)}\right] \quad (2b)$$

Equation 2a, in effect, shows that at constant temperature, the solubilization limit will depend on the relative amounts of simple and mixed micelles and their respective cholesterol binding capacities, as determined by the L/BS ratio and the parameters $A_1(T)$, $A_2(T)$, and γ. Two of these parameters are already known, $\gamma \sim 0.6$ for TC–L micelles (Mazer et al., 1980), and $A_1(T)$ has been estimated from our analysis of type 1 systems. To determine the remaining parameter, $A_2(T)$, we have fit eq 2a to the experimental values of $X_{Ch}^{max}(T)$ corresponding to L/BS = 0.6 (i.e., the value of γ).[12] We can then predict the behavior of the micellar phase boundary for 10 g/dL type 2 solutions as a function of the L/BS ratio between 0 and γ. These predictions are shown for various temperatures (4–80 °C) in Figures 13A–E and are compared with the experimental data of Carey & Small (1978). The theoretical curves provide a reasonably good fit to the data points except at very high temperatures (Figure 13D,E). The function $A_2(T)$ determined by this analysis is plotted vs. the inverse temperature in Figure 12B. Using eq 2b, one can deduce the product $K_2(S)_0(T)$ from $A_2(T)$; however, this requires an estimate of the parameter α_2, the number of cholesterol binding sites per lecithin molecule in the TC–L mixed micelle. Although lecithin bilayers can solubilize cholesterol in a maximum molar ratio of 1:1 at equilibrium[13] (Bourgès et al., 1967; Ladbrooke et al., 1968), it is likely that the ratio of cholesterol binding sites to lecithin is somewhat less than this, as these mixed micelles are presumed to have a mixed bilayer structure containing both lecithin and taurocholate (Mazer et al., 1980). From our previous results (Mazer et al., 1980), it can be estimated that the mixed micelles in 10 g/dL type 2 systems contain approximately 10 lecithin and 18 bile salt molecules (5 of which are located within the mixed bilayer). We therefore assume that such micelles can contain 5–6 cholesterol binding sites (rather than 10), and thus $\alpha_2 \simeq 0.55$. Using this value, we show in Figure 12B the temperature dependence of $K_2(T)S_0(T)$ deduced from $A_2(T)$. In comparison to $K_1(T)S_0(T)$ (Figure 12A), we find that $K_2(T)S_0(T)$ is nearly an order of magnitude larger but shows a similar 5–6-fold increase over the temperature range 4–80 °C. From the mean slope of the inverse temperature plot (Figure 12B), the enthalpy change associated with the transfer of a cholesterol molecule from the monohydrate crystal to the mixed micellar binding site is estimated to be +17.9 kJ/mol. This value is nearly identical with that found in the type 1 systems[14] and has the same magnitude and sign as the endothermic enthalpy change associated with the melting of crystalline cholesterol monohydrate, +23.9 kJ/mol (Loomis et al., 1979). This finding suggests that the processes contributing to the solubilization enthalpy, $H_{bound} - H_{ppt}$, may be similar to those involved in the disruption of crystalline cholesterol monohydrate to form the isotropic melt. To deduce the magnitude of the binding constant $K_2(T)$, we have again used the value of Saad & Higuchi (1965) for S_0(30 °C) and obtain a value for K_2(30 °C) of 1×10^7 L/mol. This implies a unitary free-energy change for the transfer of an aqueous Ch monomer to a mixed micelle site of −50.2 kJ/mol (see Appendix A), which is about 5 kJ/mol more favorable than that for the

[12] Although cholesterol monohydrate and lecithin–cholesterol liquid crystals coexist as the equilibrium precipitate phases at this molar ratio (Carey & Small, 1978), this should not seriously affect the present analysis, as both precipitates will have the same chemical potential (μ^0_{ppt}, see eq A-6).

[13] Some workers (Horwitz et al., 1971; Freeman & Finean, 1975; Lundberg, 1977) have obtained Ch/L molar ratios of 2/1 in dilute sonicated dispersions. These may represent metastable systems as discussed under section D of Discussion.

[14] These enthalpy deductions are considerably larger than those reported by Carey & Small (1978) which contain arithmetic errors in their estimation.

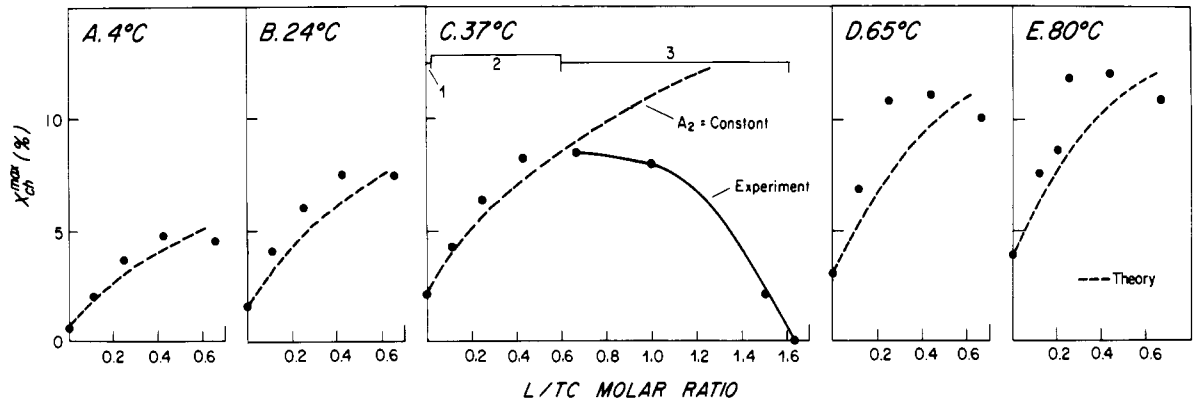

FIGURE 13: Theoretical predictions (broken curves) of X_{Ch}^{max} plotted as a function of the L/TC molar ratio in 10 g/dL type 2 systems at various temperatures (4–80 °C). Solid circles indicate the experimental data points of Carey & Small (1978) and unpublished results. In (C) (37 °C), the phase limits are extended into the regime of type 3 systems and compared with theoretical predictions that assume the parameter A_2 to remain constant. See text for explanation.

simple TC micelle binding site. The origin of this effect may be the more complete immersion of the cholesterol molecule within the mixed micelle interior, as occurs in lecithin–cholesterol bilayers (Bourgès et al., 1967; Ladbrooke et al., 1968). As seen in Figure 12B, $K_2(T)S_0(T)$ exceeds unity at temperatures greater than 50 °C, and thus the overall free energy of transferring cholesterol from the crystalline state to the mixed micellar binding site becomes favorable. In this temperature range, the occupancy of the mixed micellar sites exceeds 50% at the phase limit.

Higuchi et al. (1981) have used our quantitative model of type 2 systems (Mazer et al., 1980) to analyze the kinetics of cholesterol monohydrate dissolution into taurocholate–lecithin solutions as a function of the L/BS ratio. Their results provide strong support for the coexistence of simple and mixed taurocholate–lecithin micelles and further suggest that cholesterol uptake by simple micelles is the rate-determining step in the dissolution process. Direct evidence supporting the coexistence model is found in the equilibrium dialysis studies of TC–L systems by Duane (1977). On the other hand, Claffey & Holzbach (1981) have recently questioned this model on the basis of the small-angle X-ray scattering study of Müller (1981) and differential scanning calorimetry. While there appears to be controversy on this point, we believe that the total weight of experimental evidence supports the view that simple TC micelles coexist with TC–L mixed micelles at low L/TC ratios (0–0.6) and have shown in the present work that this picture provides a basis for quantitatively understanding the dependence of cholesterol-solubilizing capacity on L/TC ratios in type 2 systems (Figure 13).

(3) Type 3 Systems: Cholesterol Solubilization in "Mixed Disc" Micelles. As illustrated in Figure 11B, type 3 solutions contain only "mixed disc" bile salt–lecithin micelles in which cholesterol monomers can be solubilized. From eq 2a,b, it follows that in the absence of simple micelles, the dependence of $X_{Ch}^{max}(T)$ on the L/BS ratio in type 3 systems will be given by

$$X_{Ch}^{max}(T) = \frac{([L]/[BS])A_2(T)}{1 + ([L]/[BS])(1 + A_2(T))} \quad (3)$$

where $A_2(T)$ is defined by eq 2b. If we assume that the binding site parameters α_2 and $K_2(T)$ do not vary with the size of the "mixed disc" micelles and further assume that the cholesterol monomer solubility $S_0(T)$ remains the same as that in type 1 and 2 systems, it would follow that $A_2(T)$ would be independent of the L/BS ratio and identical with the function given in Figure 12B. With these assumptions, eq 3 predicts a monotonic increase in the solubilization limit which is shown in Figure 13C (T = 37 °C). It is clear that theory deviates markedly from experiment in this regime. This discrepancy can be understood, however, from the fact that the precipitate phase formed in supersaturated type 3 systems is not cholesterol monohydrate (implicitly assumed in the theoretical curve) but is instead a liquid-crystalline coprecipitate containing lecithin and cholesterol (Carey & Small, 1978). With the assumption that α_2 and $K_2(T)$ are constants for all "mixed disc" micelles, the discrepancy between the calculated and real micellar phase boundaries (Figure 13C) implies that $S_0(T)$ decreases as a function of the L/BS ratio in type 3 systems. Such behavior would be qualitatively consistent with a solubility product relationship for the lecithin–cholesterol coprecipitate, in which the chemical potential of lecithin in the system increases as a function of the L/BS ratio in type 3 systems and thus lowers the chemical potential of the cholesterol needed to coprecipitate with it. By this interpretation, the extent of cholesterol solubilization in type 3 systems would be determined by the insolubility of lecithin rather than the insolubility of cholesterol monomers as occurs in type 1 and 2 systems.

(C) Nucleation and Precipitation in Concentrated (10 g/dL) Type 1 and 2 Model Bile Systems. We first consider the metastability of 10 g/dL supersaturated type 1 solutions produced by rapid temperature changes, $T_i \rightarrow T_f$ [see section B, (1), under Results]. As shown under Appendix B, our model of cholesterol binding predicts that at the temperature T_f, the cholesterol monomer concentration, $[Ch]_{T_f}$, will exceed the solubility, $S_0(T_f)$, by the monomeric supersaturation ratio, S_1, given by

$$S_1 \equiv \frac{[Ch]_{T_f}}{S_0(T_f)} = \frac{K_1(T_i)S_0(T_i)}{K_1(T_f)S_0(T_f)} \quad (4)$$

where the product of thermodynamic factors $K_1(T)S_0(T)$ is that deduced from the solubilization analysis (Figure 12A). Using eq 4, we calculate that the largest S_1 value observed in the metastable type 1 systems was 6.8 (corresponding to X_{Ch} = 4%, T_i = 85 °C, T_f = 5 °C). Such metastability can be understood within the framework of the homogeneous nucleation theory (Walton, 1967) which defines a critical degree of monomeric supersaturation, S_1^c, below which homogeneous nucleation occurs at exceedingly slow rates and above which the nucleation rate increases dramatically. From the nucleation theory, S_1^c can be related to the unfavorable interfacial tension, σ, associated with the formation of a microprecipitate nucleus:

$$\ln S_1^c = \left[\frac{16\pi v_1^2\sigma^3}{3(kT)^3 \ln A}\right]^{1/2} \quad (5)$$

where the additional parameters are v_1 (the volume per monomer in the precipitate), kT (the thermal energy), and A [a kinetic factor which, for most purposes, is taken to equal $\sim 10^{25}$ s^{-1} cm^{-3} (Walton, 1967)]. In the case of type 1 systems, the monomerpic supersaturation of 6.8 must be less than S_1^c, from which we can deduce that σ must be greater than $\sim$12.8 erg/cm^2 for homogeneous cholesterol monohydrate nucleation. This finding is consistent with the cholesterol precipitation studies of Walton (1965), who has estimated σ to be $\sim$15 erg/cm^2 in 63% ethanol–water systems. Thus, in type 1 bile salt–cholesterol systems, homogeneous nucleation of cholesterol monohydrate cannot occur at the experimentally attainable degrees of monomeric supersaturation and must require nucleating agents (i.e., substrates which effectively reduce σ) to facilitate crystallization (heterogeneous nucleation).

In the case of 10 g/dL type 2 systems, the labile microprecipitates are not cholesterol monohydrate crystals but appear to be a nonequilibrium dispersion of liquid crystals containing cholesterol and lecithin in a molar ratio of $\sim$2:1 (Table I). This ratio is identical with the maximum Ch/L molar ratio attainable in anhydrous lecithin–cholesterol liquid crystals (Gershfeld, 1978) and in sonicated aqueous dispersions of lecithin and cholesterol (Horwitz et al., 1971; Lundberg, 1977). In our systems, the dispersed microprecipitates coalesce into macroscopic liquid crystals and at equilibrium give rise to cholesterol monohydrate (Holzbach et al., 1976; Holzbach & Corbusier, 1978; Carey & Small, 1978), consistent with the phase behavior of hydrated lecithin–cholesterol systems of the same (2/1) composition (Gershfeld, 1978).

Although the labile precipitation in 10 g/dL type 2 systems represents a nonequilibrium coprecipitation process, the observed phenomena exhibit a number of the hallmarks of single-component homogeneous nucleation [see Walton (1967)]. These include the following: (1) the existence of a metastable/labile limit (Figure 7B); (2) the dependence of the induction time, t_{ind}, on the supersaturation ratio (Figure 9A); and (3) the inverse relationship between the microprecipitate size and supersaturation ratio (Figure 9B). For this reason, we have attempted to utilize the same theory of single-component homogeneous nucleation to analyze the microprecipitation behavior of type 2 systems. To estimate the critical monomeric supersaturation, S_1^c corresponding to the metastable/labile boundary in Figure 7B, we have generalized eq 4 to type 2 systems (see Appendix B). In this case, S_1 becomes a function of both $K_1(T)S_0(T)$ and $K_2(T)S_0(T)$ evaluated at the initial (T_i) and final (T_f) temperatures. Using the data of Figure 12A,B and the T_f values corresponding to the metastable/labile limit (Figure 7B), we find that S_1^c is nearly constant, 1.93 ± 0.04, independent of T_f. From eq 5, we thus deduce the *apparent* σ value in type 2 systems to be $\sim$6.2 erg/cm^2.

An alternative means for estimating σ uses the dependence of the nucleation rate, $\dot{N}$, as a function of S_1 in the labile systems ($S_1 > S_1^c$). This dependence is theoretically predicted to obey (Walton, 1967)

$$\ln \dot{N} = \ln A - \left[\frac{16\sigma^3 v_1^2 \pi}{3(kT)^3}\right]\left[\frac{1}{(\ln S_1)^2}\right] \quad (6)$$

Thus, from the slope of the ln $\dot{N}$ vs. $1/(\ln S_1)^2$ plots, σ can be deduced. We have estimated the nucleation rates from our data by assuming that each microprecipitate particle grew from a single nucleus which formed during the induction time, t_{ind}, measured in each experiment. This assumption is consistent with the inverse relationship between $\dot{N}$ and induction time proposed by Heicklen (1976) and Neilsen (1964) and implies that $\dot{N}$ will be given by

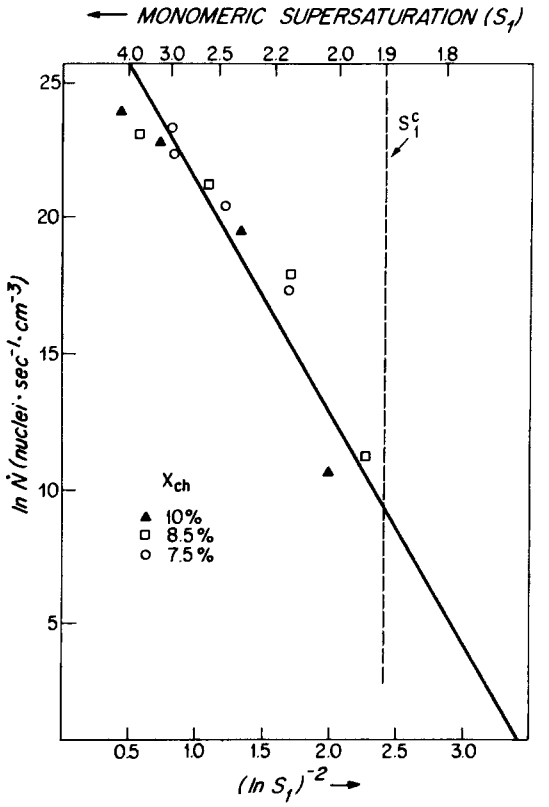

FIGURE 14: Dependence of the nucleation rate ($\dot{N}$) on the monomeric supersaturation ratio (S_1) as deduced from labile type 2 systems. Data points are plotted as ln $\dot{N}$ vs. $(\ln S_1)^{-2}$ for the purpose of deducing the interfacial tension parameter, σ, according to eq 6. See text for explanation.

$$\dot{N} \equiv \frac{1}{t_{ind}}\left[\frac{Q_{Ch}}{(4/3)\pi \bar{R}_p^3/\bar{v}_{Ch}}\right] \quad (7)$$

where the second term represents the number density of microprecipitate particles evolved in the reaction as estimated from the total amount of cholesterol precipitated (Q_{Ch}), the hydrodynamic radius of the microprecipitates ($\bar{R}_p$), and the partial molar volume of cholesterol in the precipitate ($\bar{v}_{Ch}$). Using eq 7 in conjunction with the hydrodynamic radii of the precipitates (Figure 9B) and the Q_{Ch} values given in Table I (or derived from Figure 7B), we have deduced $\dot{N}$ for the labile type 2 systems and plotted these (Figure 14) as a function of the corresponding S_1 values (see Appendix B). The $\dot{N}$ values increase by $\sim$7 orders of magnitude as S_1 increases above S_1^c and show an approximately linear variation when plotted in accordance with eq 6. From the slope of this plot, we deduce σ to be $\sim$4.4 erg/cm^2, which is comparable to that deduced previously from eq 5.

By both approaches, we have thus found that the apparent σ value in type 2 systems (4–6 erg/cm^2) is much smaller than the σ value for cholesterol monohydrate precipitation (13–15 erg/cm^2). Interestingly, the former value is comparable in magnitude to the interfacial tension of lecithin bilayers, 1–6 erg/cm^2 (Litster, 1975), consistent with the liquid-crystalline nature of the labile microprecipitates. These findings are consistent with the view that the Ch–L liquid crystal, although thermodynamically less stable than cholesterol monohydrate,

precipitates more readily from the supersaturated system by virtue of its *lower* interfacial tension. The precipitation studies of Toor et al. (1978, 1979) support this idea by showing that at high supersaturations (corresponding to our labile regime) noncrystalline amorphous precipitates are formed by homogeneous nucleation, whereas in the metastable regime the precipitation of cholesterol monohydrate occurs due to heterogeneous nucleation mechanisms.

(*D*) *Path Dependence of Microprecipitation in Dilute (3 g/dL) Type 2 Systems.* The apparent stability of the globular microdroplets formed in 3 g/dL supersaturated type 2 systems (as opposed to their coalescence in 10 g/dL systems) appears to be due to the smaller size ($\bar{R}_h \simeq$ 200–400 Å) of these particles rather than a structural or compositional difference. In addition, their very small buoyancy factor[6] slows their rate of gravitational sedimentation and phase separation. That these particles are also a nonequilibrium phase is suggested by their inability to form spontaneously when cholesterol monohydrate crystals are equilibrated with an unsaturated micellar phase at 20 °C (path C1), consistent with the view that cholesterol monohydrate is the true equilibrium precipitate in dilute supersaturated type 2 systems (as suggested in Figure 11A). Nevertheless, we have not observed the transformation of microdroplets to cholesterol monohydrate crystals in any of these dilute solutions followed for as long as 30 days. Such metastability is similar to that seen in the sonicated "2/1 cholesterol/lecithin" systems (Lundberg, 1977) and may be another manifestation of the high σ value associated with the homogeneous nucleation of cholesterol monohydrate in aqueous systems.

Our studies show that the stable microdroplets form by paths that pass through a supersaturated micellar state in which excess cholesterol is present both as monomers and as bound to the micelle. Examples of this mechanism include temperature change experiments[15] and the dilution of the concentrated micellar phase at 70 °C (path B).[16] While these paths appear to illustrate the "sufficient" conditions for microdroplet formation, they do not provide paths that are necessarily relevant to the in vivo conditions of hepatic bile formation. However, paths D_1 and D_2, in which bile salt solutions were mixed with hydrated and anhydrous Ch–L systems, provide conditions that may be similar to the interaction of bile salts, lecithin, and cholesterol at the intracellular or canalicular membrane sites of bile formation (Jones et al., 1980; Graham et al., 1981). In both cases, microdroplet particles were formed, suggesting that the solubilization of the lecithin–cholesterol bilayers by bile salts creates a transiently supersaturated micellar phase which can give rise to the stable microdroplets.

(*E*) *Conclusions and Pathophysiologic Implications.* The present studies offer a number of new insights into the molecular interactions of the biliary lipids that are significant from the physicochemical viewpoint and have potentially important pathophysiological implications.

In the case of unsaturated model bile systems, our studies of both dilute (3 g/dL) and concentrated (10 g/dL) solutions have shown that the solubilization of cholesterol has little influence on the size, structure, and growth of simple and mixed micellar aggregates formed in the absence of cholesterol (Mazer et al., 1979, 1980). These findings suggest that unsaturated hepatic and gallbladder bile, whose L/BS ratios and total lipid concentrations correspond to type 2 model systems (Carey & Small, 1978), should contain both simple (bile salt–cholesterol) and mixed (bile salt–lecithin–cholesterol) micelles. The sizes and relative amounts of the two species will depend on the bile salt species, the L/BS ratio, and the total lipid concentration (Mazer et al., 1980) but, in general, should fall between 10 and 35 Å, as found in the TC–L system. Whether such micellar structures actually exist at the hepatocellular sites of bile secretion cannot be inferred from the present work, as there is no direct information yet available on the relative and total lipid concentrations of canalicular bile (Erlinger, 1981). In particular, estimates of the water content of canalicular bile, which are still uncertain (Javitt, 1976), are vital for determining whether the biliary lipids are secreted as a type 2 micellar system, as large "mixed disc" micelles (type 3), or in vesicular structures as might occur in very dilute systems (Mazer et al., 1981).

In conjunction with the present experimental findings, we have offered a theoretical interpretation of the micellar phase boundary in model bile systems, based on a quantitative model of cholesterol binding to simple and mixed micelles. Our theory explains the origin of the micellar phase boundary as an equilibrium between bound and precipitated cholesterol that involves the aqueous monomer as an intermediate. In type 1 and 2 systems, where cholesterol monohydrate is the equilibrium-precipitated phase, it is shown that the marked temperature dependence of the phase boundary is a reflection of the large enthalpy change (~18 kJ/mol) associated with the transfer of cholesterol from the monohydrate crystal to the micellar binding sites. In type 3 systems, the cholesterol "precipitate" is a liquid-crystalline or vesicle phase which contains lecithin and cholesterol.

The behavior of supersaturated systems displays a number of features that may have important pathophysiologic relevance. In the case of dilute (3 g/dL) type 2 systems, we have observed the presence of small globular microdroplets 200–400 Å in radius which remain dispersed in solution at cholesterol mole fractions (10–15%) typical of the cholesterol contents found in the hepatic bile of cholesterol gallstone patients and of normal patients, whose hepatic bile is often supersaturated (Holzbach et al., 1973; Carey & Small, 1978). These microdroplets are not cholesterol monohydrate crystals but instead contain cholesterol and lecithin in a Ch/L molar ratio of approximately 2/1. We have further shown that such particles form spontaneously when bile salt solutions are mixed with multilamellar dispersions of lecithin and cholesterol, a process that may resemble events taking place at intracellular and/or canalicular membranes (Jones et al., 1980; Graham et al., 1981). On this basis, we suggest[17] that the microdroplets may be formed in vivo and provide a second vehicle (in addition to the micelles) for transporting cholesterol within the biliary tree. The finding that the microdroplets remain stable and do not evolve into cholesterol monohydrate crystals, in vitro, may help to explain why cholesterol gallstones do not form in the proximal biliary tree despite high degrees of cholesterol supersaturation.

The behavior of 10 g/dL supersaturated type 2 systems has relevance to the properties of lithogenic gallbladder bile. Using temperature change studies, we have confirmed the existence

[15] An example of this path is the system with X_{Ch} = 7% which is a micellar phase at 60 °C but reversibly forms "stable" microdroplets at 20 °C (see Figure 4B).

[16] The formation of microdroplets by path C2 can also be understood in this way, since incubation at 90 °C permits greater Ch solubilization and thus leads to a supersaturated micellar phase when the temperature is returned to 20 °C.

[17] Robins & Armstrong (1976) have previously speculated that biliary cholesterol could be transported in liquid-crystalline dispersions with lecithin.

of a metastable/labile supersaturation limit (Carey & Small, 1978) below which the micellar phase remains metastably supersaturated with cholesterol. Above this limit, which corresponds to a supersaturation ratio of ~1.6, the systems form large globular microprecipitates whose mean radii range from 500 to greater than 10000 Å, varying inversely with the degree of supersaturation. The composition of these microprecipitates is similar to those found in the dilute type 2 systems (i.e., Ch/L molar ratio of ~2/1). However, in contrast to the dilute systems, the large microprecipitates coalesce into a macroscopic liquid-crystalline phase and subsequently are transformed into cholesterol monohydrate crystals. These observations are similar to those of Holzbach and co-workers (Holzbach et al., 1976) and suggest that the labile microprecipitates, rather than being "embryonic gallstones" (Mazer et al., 1978), represent a nonequilibrium phase which may in fact delay the true crystallization process (Holzbach et al., 1976; Holzbach & Corbusier, 1978). The present studies further suggest that the homogeneous nucleation of pure cholesterol monohydrate in supersaturated type 2 systems cannot occur at the attainable degrees of supersaturation either in vitro or in vivo due to the high value of the Ch–L solvent interfacial tension, σ (13–15 erg/cm^2). On the other hand, the liquid-crystalline precipitates can form by homogeneous nucleation due to their smaller σ value (4–6 erg/cm^2). These findings point to the potential importance of nucleating or antinucleating factors (Small, 1980; Sedaghat & Grundy, 1980; Holan et al., 1979; Lee et al., 1981) which could influence the rate of heterogeneous nucleation of cholesterol monohydrate from the metastable state or affect its rate of conversion from the liquid-crystalline phase. In attempting to identify such factors in native bile, we believe that the present studies could provide a useful experimental and theoretical framework.

Acknowledgments

We gratefully acknowledge the technical assistance of Grace Ko, the secretarial assistance of Rebecca Ankener, Claire Supple, and John Shackett, the artistic talent of Jean Kanski, and the expertise of Dr. Marcia Armstrong and Erica Hartweig, who performed the electron micrograph studies. We are also indebted to Professor George Benedek of M.I.T. for the use of his laser light scattering facilities and for his interest in this work and to Dr. Mark Stecher for stimulating discussions on micellar thermodynamics. N.A.M. thanks the Connecticut Mutual Life Insurance Company for sponsoring an Insurance Medical Scientist Scholarship (1976–1978).

Appendix

(*A*) *Quantitative Theory of Cholesterol Solubilization for Type 1 and 2 Systems.* We consider first type 1 systems where cholesterol monomers, Ch, are in reversible equilibrium with molecules that are bound to simple bile salt micelles. Let M_1 represent the unoccupied type 1 binding site and M_1·Ch a bound cholesterol molecule. At equilibrium, the concentrations of all three species are related through the law of mass action (Moore, 1972):

$$[M_1\cdot Ch] = K_1(T)[M_1][Ch] \qquad (A\text{-}1)$$

where $K_1(T)$ is the binding constant which can be expressed in terms of the standard chemical potentials of all three species by

$$K_1(T) = \exp\{-[\mu^0_{M_1\cdot Ch} - (\mu^0_{Ch} + \mu^0_{M_1})]/(RT)\} \qquad (A\text{-}2)$$

The conservation of material constraints relate the equilibrium concentrations to the total concentration of cholesterol, $[Ch]_0$, and binding sites, $[M_1]_0$, in the system:

$$[Ch]_0 = [Ch] + [M_1\cdot Ch] \qquad (A\text{-}3a)$$

$$[M_1]_0 = [M_1] + [M_1\cdot Ch] \qquad (A\text{-}3b)$$

The value of $[M_1]_0$ can in turn be related to the total bile salt concentration, $[BS]_0$:

$$[M_1]_0 = \alpha_1([BS]_0 - CMC) \qquad (A\text{-}4)$$

where α_1 is the ratio of Ch binding sites to BS molecules in the micelle and CMC is the bile salt monomer concentration in equilibrium with the micelles. In the limit of high concentration (i.e., 10 g/dL), the CMC can be neglected in eq A-4 and together with the previous equations implies that the concentration of solubilized molecules, $[M_1\cdot Ch]$, will be related to the monomer concentration, [Ch], by

$$[M_1\cdot Ch] = \alpha_1[BS]_0\left[\frac{K_1(T)[Ch]}{1 + K_1(T)[Ch]}\right] \qquad (A\text{-}5)$$

From this result, the maximum degree of solubilization will be attained when [Ch] reaches its maximum value, and this will correspond to the aqueous solubility of the monomer, denoted $S_0(T)$. For monomer concentrations above $S_0(T)$, the excess cholesterol will form a precipitate (at equilibrium) whose standard chemical potential, μ^0_{ppt}, determines the value of $S_0(T)$ according to

$$S_0(T) = \exp\{-[\mu^0_{Ch} - \mu^0_{ppt}]/(RT)\} \qquad (A\text{-}6)$$

Here, $S_{0(T)}$ is given in dimensionless units normalized by the molarity of the solvent.

To calculate the quantity $X_{Ch}^{max}(T)$, corresponding to the solubilization limit, we compute the mole fraction $[Ch]_0/([BS]_0 + [Ch]_0)$, by using eq A-5 with $S_0(T)$ in place of [Ch] and ignoring the monomer concentration in eq A-3a. The result simplifies to

$$X_{Ch}^{max}(T) = \frac{\alpha_1\{K_1(T)S_0(T)/[1 + K_1(T)S_0(T)]\}}{1 + \alpha_1\{K_1(T)S_0(T)/[1 + K_1(T)S_0(T)]\}} \qquad (A\text{-}7)$$

which is identical with eq 1a,b in the text. From the present derivation, one can also express the product $K_1(T)S_0(T)$ appearing in eq A-7 in terms of chemical potentials by using eq A-2 and A-6:

$$K_1(T)S_0(T) = \exp\{-[\mu^0_{M_1\cdot Ch} - (\mu^0_{M_1} + \mu^0_{ppt})]/(RT)\} \qquad (A\text{-}8)$$

This result shows that $K_1(T)S_0(T)$ reflects the free-energy change associated with the transfer of a cholesterol molecule from the precipitate to the M_1 binding site. It also follows from eq A-8 that the temperature dependence of $K_1(T)S_0(T)$ can be related to the partial molar enthalpy change, $H_{bound} - H_{ppt}$, associated with the transfer of cholesterol from the precipitate to the bound state. This enthalpy difference is derived from the general Gibbs–Helmholtz equation (Moore, 1972) and in the present case can be expressed as

$$H_{bound} - H_{ppt} = -R\frac{\partial \ln [K_1(T)S_0(T)]}{\partial(1/T)} \qquad (A\text{-}9)$$

It is this relationship which has been used to deduce the enthalpy changes given in the text from the data of Figure 12.

In the case of type 2 systems, cholesterol molecules can be bound to both simple micelles and mixed bile salt–lecithin micelles. Denoting the binding sites in the latter aggregates as M_2 sites, it follows by analogy with the previous derivation that the maximum cholesterol concentration solubilized in the mixed micelles will be given by

$$[M_2\cdot Ch] = \alpha_2[L]_0\left[\frac{K_2(T)S_0(T)}{1 + K_2(T)S_0(T)}\right] \quad (A\text{-}10)$$

where α_2 is the ratio of M_2 sites to lecithin molecules in the mixed micelle, $[L]_0$ is the total concentration of lecithin in the system, and $K_2(T)$ is the binding constant for the M_2 site. To calculate the solubilization limit, $X_{Ch}^{max}(T)$, we must add the contributions from both the M_1 and M_2 sites:

$$X_{Ch}^{max}(T) = \frac{[M_1\cdot Ch] + [M_2\cdot Ch]}{[BS]_0 + [L]_0 + [M_1\cdot Ch] + [M_2\cdot Ch]} \quad (A\text{-}11)$$

where we have again ignored the contribution of the cholesterol monomers, which is negligibly small. To calculate $[M_1\cdot Ch]$ for the case of type 2 systems, we must modify eq A-4 and A-5 to take account of the fact that not all of the bile salts are used to make simple micelles. According to our previous analysis of the coexistence of simple and mixed micelles (Mazer et al., 1980), the concentration of bile salts involved in simple micelle formation will equal $[BS]_0 - \gamma^{-1}[L]_0 - IMC$, where γ corresponds to the L/BS ratio in the mixed micelles which form over the coexistence regime and IMC is the bile salt monomer concentration in equilibrium with both simple and mixed micelles. At 10 g/dL concentrations, we can neglect the IMC term and thus replace $[BS]_0$ by $[BS]_0 - \gamma^{-1}[L]_0$ in eq A-5. At the solubilization limit, the quantity $[M_1\cdot Ch]$ will thus be given by

$$[M_1\cdot Ch] = \alpha_1([BS]_0 - \gamma^{-1}[L]_0)\left[\frac{K_1(T)S_0(T)}{1 + K_1(T)S_0(T)}\right] \quad (A\text{-}12)$$

Substituting eq A-10 and A-12 into A-11 and simplifying, one obtains the result given as eq 2a,b in the text.

It should be noted here that the binding constant $K_2(T)$ can be expressed in terms of the standard chemical potentials of M_2 and $M_2\cdot Ch$ in analogy with eq A-2 and that the product $K_2(T)S_0(T)$ is likewise a reflection of the transfer of a cholesterol molecule from the precipitate to the M_2 site, in analogy with eq A-8. Similarly, one can deduce the enthalpy change associated with solubilization at the M_2 sites from the temperature dependence of $K_2(T)S_0(T)$ in analogy with eq A-9.

(B) Deductions of the Monomeric Supersaturation (S_1) in Type 1 and Type 2 Systems. In a system containing total concentrations of $[M_1]_0$ and $[M_2]_0$ binding sites, respectively, the maximum amount of cholesterol, $[Ch]_0$, which can be solubilized at an initial temperature, T_i, will be given by eq A-5 and A-10 as

$$[Ch]_0 = [M_1]_0\left[\frac{K_1(T_i)S_0(T_i)}{1 + K_1(T_i)S_0(T_i)}\right] + [M_2]_0\left[\frac{K_2(T_i)S_0(T_i)}{1 + K_2(T_i)S_0(T_i)}\right] \quad (B\text{-}1)$$

where $K_1(T)$ and $K_2(T)$ are the equilibrium binding constants for the M_1 and M_2 binding sites and $S_0(T)$ is the monomeric solubility of cholesterol. If the solution temperature is lowered to T_f, a shift in the relative amounts of bound and monomeric cholesterol will occur (prior to precipitation). The resulting monomeric concentration, $[Ch]_{T_f}$, must satisfy

$$[Ch]_0 = [M_1]_0\left[\frac{K_1(T_f)[Ch]_{T_f}}{1 + K_1(T_f)[Ch]_{T_f}}\right] + [M_2]_0\left[\frac{K_2(T_f)[Ch]_{T_f}}{1 + K_2(T_f)[Ch]_{T_f}}\right] \quad (B\text{-}2)$$

where the quantity $[Ch]_0$ has the value given by eq B-1.

Since the degree of monomeric supersaturation, S_1, corresponds to the ratio $[Ch]_{T_f}/[S_0(T_f)]$, we can rewrite eq B-2 in terms of S_1 as

$$[Ch]_0 = [M_1]_0\left[\frac{K_1(T_f)S_0(T_f)S_1}{1 + K_1(T_f)S_0(T_f)S_1}\right] + [M_2]_0\left[\frac{K_2(T_f)S_0(T_f)S_1}{1 + K_2(T_f)S_0(T_f)S_1}\right] \quad (B\text{-}3)$$

Equating the right-hand sides of eq B-1 and B-3, it follows that the S_1 value created by the temperature change ($T_i \rightarrow T_f$) will be a function of the relative numbers of M_1 and M_2 sites in solutions and on the products $K_1(T)S_0(T)$ and $K_2(T)S_0(T)$ evaluated at both temperatures. In the case of type 1 systems containing only M_1 sites, the equations simplify so that S_1 will be given by

$$S_1 = \frac{K_1(T_i)S_0(T_i)}{K_1(T_f)S_0(T_f)} \quad (B\text{-}4)$$

as given in eq 4 of the text. In the case of type 2 systems, where both M_1 and M_2 sites are present, S_1 will depend in a more complex fashion on the products $K_1(T)S_0(T)$ and $K_2(T)S_0(T)$ evaluated at both T_i and T_f. Using the temperature dependence of these products given in Figure 12, we have obtained the S_1 values corresponding to the metastable/labile phase boundary and the labile type 2 systems given in section C under Discussion.

Registry No. Ch, 57-88-5; TC, 145-42-6.

References

Admirand, W. H., & Small, D. M. (1968) *J. Clin. Invest. 47*, 1043.

Bourgès, M., Small, D. M., & Dervichian, D. G. (1967) *Biochim. Biophys. Acta 144*, 189.

Carey, M. C., & Small, D. M. (1970) *Am. J. Med. 49*, 590.

Carey, M. C., & Small, D. M. (1978) *J. Clin. Invest. 61*, 998.

Carey, M. C., Montet, J.-C., Phillips, M. C., Armstrong, M. J., & Mazer, N. A. (1981) *Biochemistry 20*, 3637.

Claffey, W. J., & Holzbach, R. T. (1981) *Biochemistry 20*, 415.

Corrigan, O. I., Su, C. C., Alkan, M. H., Higuchi, W. I., & Hofmann, A. F. (1980) *J. Pharm. Sci. 69*, 869.

Duane, W. C. (1977) *Biochem. Biophys. Res. Commun. 74*, 223.

Erlinger, S. (1981) *Hepatology 1*, 352.

Feldman, E. B., & Borgström, B. (1966) *Lipids 1*, 430.

Forker, E. L. (1979) in *Gallstones* (Fisher, M. M., Goresky, C. A., Shaffer, E. A., & Strasberg, S. M., Eds.) p 35, Plenum Press, New York.

Freeman, R., & Finean, J. B. (1975) *Chem. Phys. Lipids 14*, 313.

Fromm, H., Amin, P., Klein, H., & Kupke, I. (1980) *J. Lipid Res. 21*, 259.

Gershfeld, N. L. (1978) *Biophys. J. 22*, 469.

Gilbert, D. B., & Reynolds, J. A. (1976) *Biochemistry 15*, 71.

Graham, J. M., Bird, R., & Northfield, T. C. (1981) *Gastroenterology 80*, 1162.

Gurantz, D., Laker, M. F., & Hofmann, A. F. (1981) *J. Lipid Res. 22*, 373.

Hall, C. E. (1953) *Introduction to Electron Microscopy*, p 318, McGraw-Hill, New York.

Hardison, W. G. M., & Apter, J. T. (1972) *Am. J. Physiol. 222*, 61.

Heicklen, J. (1976) *Colloid Formation and Growth*, Academic Press, New York.

Higuchi, W. I., Su, C. C., Park, J. Y., Alkan, M. H., & Gulari, E. (1981) *J. Phys. Chem. 85*, 127.
Holan, K. R., Holzbach, R. T., Hermann, R. E., Cooperman, A. M., & Claffey, W. J. (1979) *Gastroenterology 77*, 611.
Holzbach, R. T., & Marsh, M. (1975) *Mol. Cryst. Liq. Cryst. 28*, 217.
Holzbach, R. T., & Corbusier, C. (1978) *Biochim. Biophys. Acta 528*, 436.
Holzbach, R. T., Marsh, M., Olszewski, J., & Holan, K. (1973) *J. Clin. Invest. 52*, 1467.
Holzbach, R. T., Corbusier, C., Marsh, M., & Naito, H. K. (1976) *J. Lab. Clin. Med. 87*, 987.
Horwitz, C., Krut, L., & Kaminsky, L. (1971) *Biochim. Biophys. Acta 239*, 329.
Igimi, H., & Carey, M. C. (1981) *J. Lipid Res. 72*, 254.
Jandacek, R. J., Webb, M. R., & Mattson, F. H. (1977) *J. Lipid Res. 18*, 203.
Javitt, N. B. (1976) *N. Engl. J. Med. 295*, 1464.
Jones, A. L., Schmuker, D. L., Renston, R. H., & Murakami, T. (1980) *Dig. Dis. Sci. 25*, 609.
Koppel, D. E. (1972) *J. Chem. Phys. 57*, 4814.
Ladbrooke, B. D., Williams, R. M., & Chapman, D. (1968) *Biochim. Biophys. Acta 150*, 333.
Lee, S. P., LaMont, J. T., & Carey, M. C. (1981) *J. Clin. Invest. 67*, 1712.
Litster, J. D. (1975) *Phys. Lett. A 53A*, 193.
Loomis, C. R., Shipley, G. G., & Small, D. M. (1979) *J. Lipid Res. 20*, 525.
Lundberg, B. (1977) *Chem. Phys. Lipids 18*, 212.
Mazer, N. A. (1978) Ph.D. Thesis, Massachusetts Institute of Technology, Cambridge, MA.
Mazer, N. A., Benedek, G. B., & Carey, M. C. (1976) *J. Phys. Chem. 80*, 1075.
Mazer, N. A., Benedek, G. B., & Carey, M. C. (1978) *Gastroenterology 74*, 1173.
Mazer, N. A., Carey, M. C., Kwasnick, R. F., & Benedek, G. B. (1979) *Biochemistry 18*, 3064.
Mazer, N. A., Benedek, G. B., & Carey, M. C. (1980) *Biochemistry 19*, 601.
Mazer, N. A., Schurtenberger, P., Carey, M. C., Känzig, W., & Preisig, R. (1981) *Gastroenterology 80*, 1314.
Missel, P. J., Mazer, N. A., Benedek, G. B., Young, C. Y., & Carey, M. C. (1980) *J. Phys. Chem. 84*, 1044.
Moore, W. J. (1972) *Physical Chemistry*, Prentice-Hall, Englewood Cliffs, NJ.
Mukerjee, P., & Cardinal, J. R. (1976) *J. Pharm. Sci. 65*, 882.
Müller, K. (1981) *Biochemistry 20*, 404.
Neilsen, A. E. (1964) *Kinetics of Precipitation*, MacMillan, New York.
Newman, G. C., & Huang, C. H. (1975) *Biochemistry 14*, 3363.
Oh, S. Y., McDonnell, M. E., Holzbach, R. T., & Jamieson, A. M. (1977) *Biochim. Biophys. Acta 488*, 25.
Robins, S. J., & Armstrong, M. J. (1976) *Gastroenterology 70*, 397.
Saad, H. Y., & Higuchi, W. I. (1965) *J. Pharm. Sci. 54*, 1205.
Salvioli, G., Igimi, H., & Carey, M. C. (1981) *Gastroenterology 80*, 1268.
Sedaghat, A., & Grundy, S. M. (1980) *N. Engl. J. Med. 302*, 1274.
Shaffer, E. A., & Small, D. M. (1976) *Current Problems in Surgery*, Vol. XIII, No. 7, p 1.
Small, D. M. (1967) *Gastroenterology 52*, 607.
Small, D. M. (1968) *Adv. Chem. Ser. No. 84*, 31.
Small, D. M. (1971) in *The Bile Acids* (Nair, P. P., & Kritchevsky, D., Eds.) Vol. 1, p 249, Plenum Press, New York.
Small, D. M. (1980) *N. Engl. J. Med. 302*, 1305.
Toor, E. W., Evans, D. F., & Cussler, E. L. (1978) *Proc. Natl. Acad. Sci. U.S.A. 75*, 6230.
Toor, E. W., Evans, D. F., & Cussler, E. L. (1979) in *Gallstones* (Fisher, M. M., Goresky, C. A., Shaffer, E. A., & Strasberg, S. M., Eds.) p 169, Plenum Press, New York.
Vitello, L. (1971) Ph.D. Thesis, Clarkson College, New York.
Walton, A. G. (1965) *International Symposium on Nucleation Phenomena*, Cleveland, OH, April 7–9, 1965, Abstracts of the Proceedings, p 24.
Walton, A. G. (1967) *The Formation and Properties of Precipitates*, Interscience, New York.
Woodford, F. P. (1969) *J. Lipid Res. 10*, 539.
Young, C. Y., Missel, P. J., Mazer, N. A., Benedek, G. B., & Carey, M. C. (1978) *J. Phys. Chem. 82*, 1375.